EF Nr. 195124

Bundesamt für Energiewirtschaft
Office fédéral de l'énergie
Ufficio federale dell'energia
Uffizi federal d'energia

Research programme on
ambient heat, waste heat and cogeneration
of the Swiss Federal Office of Energy

Performances of 3.9 MW_{th} Ammonia Heat Pumps within a District Heating Cogeneration Power Plant

Status after eleven Years of Operation

Prepared by
X.Pelet, Prof.Dr.D.Favrat
Laboratory for Industrial Energy Systems
Swiss Federal Institute of Technology of Lausanne, 1015 Lausanne
and
A.Vögeli, Sulzer Friotherm AG, 8401 Winterthur

on behalf of the
Swiss Federal Office of Energy

November 1997 Final Report

Abstract

Key words: natural refrigerant, ammonia, heat pump, cogeneration, screw compressor, district heating

A complex heating and cogeneration plant including two 3.9 MWth ammonia heat pumps and two 3 MWel gas turbines with heat recovery boilers and three storage tanks of 66 GJ has been in operation since 1986. The heating surface is actually about 280'000 m^2 and is still increasing. It is divided into two parts, a medium and low-temperature district heating network. To optimise on the best possible performance from the heat pumps, the network water is delivered directly to the radiators of the building without intermediate heat exchangers. This plant is still a pioneer installation for many of its characteristics. This report is a result of an experimental evaluation during the eleventh season of heating. Energy balances of the whole plant throughout the season are discussed as well as the performances of one fully instrumented heat pump. Results confirm the interest of this type of technology combination even if the performances of the heat pump exhibit a decrease of COP from an average of 5 to about 4.4. This drop is mainly attributed to a drop in compressor performance, fouling in the evaporator, and the presence of inert gases.

Résumé

Mots clefs: réfrigérant naturel, ammoniac, pompe à chaleur, cogénération, compresseur à vis, réseau de chauffage

Un complexe de chauffage et de cogénération incluant deux pompes à chaleur à ammoniac de 3.9 MWth et deux turbines à gaz de 3 MWel avec une récupération de la chaleur et trois accumulateurs de chaleurs de 66 GJ sont en opération depuis 1986. La surface actuelle de chauffage est à peu prés de 280'00 m^2 et ne cesse d'augmenter. Elle est divisée en deux parties, un réseau moyenne température et un réseau basse température. Afin d'améliorer les performances de ce réseau, l'eau de chauffage est délivrée directement aux radiateurs des bâtiments sans échangeurs intermédiaires. Cette installation est toujours actuellement à la pointe pour plusieurs de ces caractéristiques. Ce rapport est le résultat de tests fait durant la onzième année de chauffage. Différentes efficacité durant la saison sont discutées aussi bien que les performances d'une des deux pompes à chaleur complètement équipée d'appareils de mesure. Les résultats confirment l'intérêt pour de tel type de technologie combinant deux systèmes malgré la diminution d'efficacité moyenne de 5 à peu prés 4.4. Cette diminution est principalement attribuée à une chute de performance du compresseur, à un encrassement de l'évaporateur et la présence de gaz inertes.

Zusammenfassung

Suchbegriffe: natürliche Kältemittel, Ammoniak, Wärmepumpe, Kraft-Wärme-Kopplung, Schraubenkompressor, Heizsystem

Ein Heizungssystem mit Kraft-Wärme-Kopplung mit zwei 3.9 MWth Wärmepumpen und zwei 3 MWel Gasturbinen mit Wärmerückgewinnung und drei 66 GJ Wärmespeichern ist seit 1986 in Betrieb. Die momental damit beheizte Fläche beträgt ungefähr 280'000 m^2, doch diese Fläche vergrößert sich ständig. Das Heizsystem besteht aus zwei Teilen, einem Mittel- und einem Tieftemperaturbereich. Um die Leistung zu verbessern sind die Heizkörper direkt an das Netz angeschlossen, d.h. es befindet sich kein Wärmetauscher dazwischen.

This project has been supported by the Swiss Federal Office of Energy. The Swiss Federal Office of Energy assumes no responsability for the content and the conclusions of this report.

In vielen Teilbereichen ist die Anlage eine Pilotanlage, d.h. weltweit einzigartig. Dieser Bericht ist das Ergebnis der Messungen die während des elften Betriebsjahres der Anlage durchgeführt wurden. Die Bandbreite der Wirkungsgrade während des elften Betriebsjahres wird ebenso diskutiert wie die Leistung einer der zwei Wärmepumpen, welche vollständig mit Meßgeräten ausgerüstet ist.

Die Resultate bestätigen das Interesse für diese Art Technologie, welche zwei Heizsysteme miteinander koppelt, auch wenn der Wirkungsgrad der Wärmepumpe von 5 auf ungefähr 4.4 absank. Diese Verringerung beruht hauptsächlich auf einem Leistungsrückgang des Kompressors, der Verunreinigung des Verdampfers und der Anwesenheit inerten Gases im Kreislauf.

OFEN Report

Project *N°19326*

TABLE OF CONTENTS

Appendix

1. INTRODUCTION

1.1 Generality

As a substitute for synthetic refrigerant such as CFC or HCFC, the ammonia (NH_3) as a natural refrigerant is progressively rediscovered in spite of its toxicity and its flammability. This phenomenon is due to many different factors: the ammonia is cheap, has good thermodynamic properties and has no effects for the destruction of the ozone layer, and neither global warming [1]. Different technologies have appeared to facilitate the use of ammonia within good margins of safety. Dramatically reduced charges and continuous development of components and systems have been crucial for the renewed interest in ammonia. Examples of important new technologies are:

- Packaged, low charge liquid chillers
- 40 bar open, reciprocating compressors and 25 bar semi-hermetic compressors
- Welded, semi-welded and nickel brazed plate heat exchangers
- Plate-and-shell heat exchangers
- Miscible lubricants (polyalkylene glycol, PAG)
- DX-systems (direct expansion evaporators and electronic expansion valves/injectors)
- Safety systems (leak detectors, alarm systems, ammonia scrubbers etc.)

The Swiss Federal Institute of Technology of Lausanne (EPFL) has a power plant consisting of two ammonia heat pumps rated 3.9 MWth each, two gas turbines each rated 3 MWel / 6 MWth and three hot water storage tanks (Figure 1). Since 1986, buildings of the Swiss Federal Institute of Technology of Lausanne (EPFL) have been heated by this plant. The plant is located in a separate building than the university buildings. Note that the plant is run automatically without continuous presence of an operator.

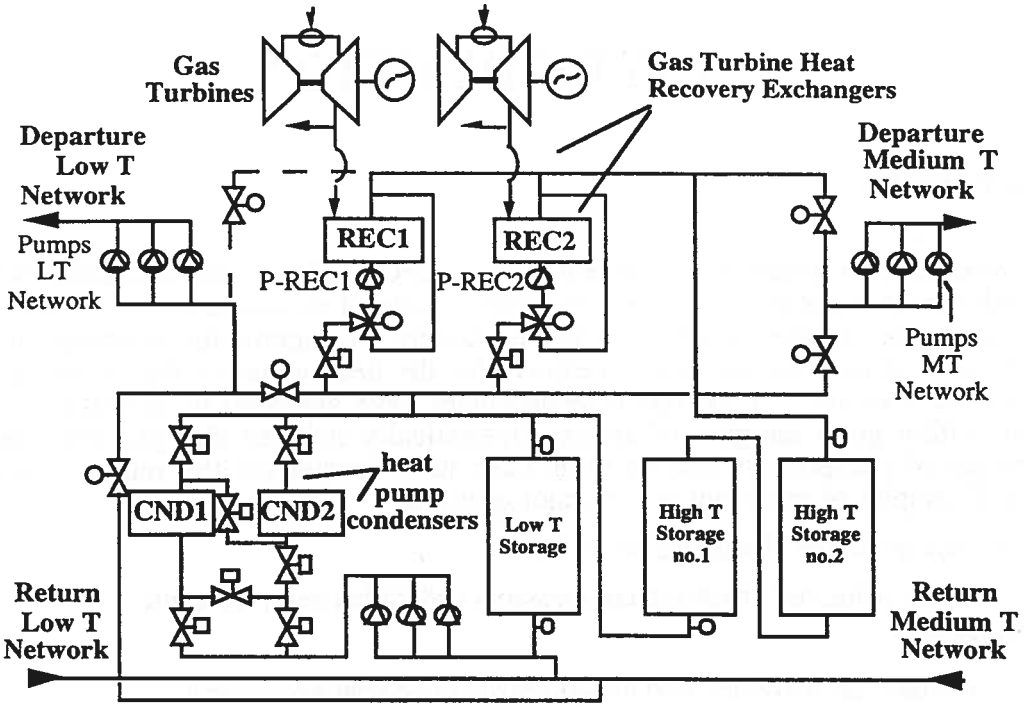

Figure 1: General layout of the heating plant at the EPFL (CCT).

Both heat pumps are identical and use ammonia as a working fluid, a choice which was made at the time mainly with regard to of the excellent thermodynamic properties of ammonia. Each is equipped with one electrically driven oil-injected screw compressor with an economizer port. The heat source for the evaporator is water pumped from Lake Leman, 1 km away. The water is taken at a 65 m depth, some 700 m offshore. The water, cooled of the order of 3°C in the evaporator, is then released into a nearby river "La Sorge". The condensers of the two heat pumps can work alone, in parallel, or in series depending upon the heating load [2]. These two heat pumps were designed and constructed by Sulzer.

Each gas turbine is connected to its own electrical generator, so operation of the gas turbines is decoupled from the heat pumps. Since the commissioning of the plant the gas turbines have been using light fuel oil but plans are to run with natural gas in the future to meet more stringent environmental regulations, except for the periods of peak gas demands when oil will still be used.

It was initially planned to use the gas turbines mainly for peak shaving, for heating the storage buffer tanks used for temperature regulation and for boosting the network temperature when the outdoor temperature drops below 0°C. However, recent increases in the daily electrical utility rates as well as the increase of the heat demand with new buildings being connected, have introduced new conditions for operating the plant. A thermoeconomic model has been developed to optimise the plant using a mixed integer linear programming approach but results have not yet been fully integrated [3].

One of the heat pump is completely instrumented with measures of pressure, temperature, and mass flow. Experimental data and analysis of the major components in different operation modes are presented here. Measurements have been collected at regular intervals during the heating period 1996-1997.

1.2 Objective

The initial goals of the project were:

- "Make a scientific study of the heat plant of the EPFL and more precisely of the behaviour and the performances of the heat pump of 3.9 MWth that is fully instrumented. This study includes:
- The heat load curve during the cold period, with the measurement of the atmospheric temperature
- An analysis of the total efficiency of the heat pumps in the context of the actual strategy of distribution of the load between the gas turbines and the heat pumps (warning: this strategy established on an economical base can not be influenced by the present project)
- A detailed study of the performances of the instrumented heat pump with energy balances on the different components (evaporator, condenser, compressor)
- A preanalysis of the improvements (performances, reduction of load) in case of realisation of future other similar plants.

1.3 Processes

This report is divided into two main parts. The first one concerns the plant. Daily collection of the plant meters of the plant was made. Different analyse were made showing the evolution of the consumption and of the production of the plant during the heating period 1996-1997.

The second part concerns the heat pumps n°2. This heat pump is instrumented with temperature and pressure sensors as well as flow meters. A Lab View program facilitates the data acquisition. An other program made by the Laboratory for Industrial Energetic of the EPFL (LENI-EPFL) calculates the efficiencies of the different components of the heat pump. Stability of the heat pump regime was ensured by an engineer of Sulzer during the tests made at different loads. Finally these tests were compared to twenty five tests made by Sulzer just before the commissioning of the installation. These tests cover different outside conditions and different modes of operation: with or without an economizer port. The present tests made during the 1997 winter included only operation with the economizer port active.

2. THE PLANT

2.1 Meters

During measurement campaign two ways of acquisition have been used. During the first period, reading have been made manually twice a day. During the second period, a computer program was used to take measurements every 15 minutes. The heating period began the 1st October 1996 till the 5th May 1997.

Table 1: List of the different meters of the plant

Name of the meters	Measures	Comments
TP1 Thermopump 1	kWh	Electrical consumption of the compressor of the heat pump 1
TP2 Thermopump 2	kWh	Electrical consumption of the compressor of the heat pump 2
TG1 Gas turbine 1	kWh day [1] kWh night [2]	Electrical production of the gas turbine 1
TG2 Gas turbine 2	kWh day [1] kWh night[2]	Electrical production of the gas turbine 2
F+L A Force light A	kWh	Electrical consumption of all apparatus of the CCT (pumps, computer driven, light,...) except for the compressors of the heat pumps. This meter also measures the Pumps Boosters consumption
F+L B Force light B	kWh	Same function as the meter F+L A, is used as a backup in case of interruption of the F+L A meter
Heating oil TG1	Tonnes	Heating oil consumption of the gas turbine 1
Heating oil TG2	Tonnes	Heating oil consumption of the gas turbine 2
E.L. TP1+TP2 Lake water TP1 and TP2	m^3	Water consumption of the lake water used in the evaporators of the heat pumps
E.I. EPFL1 Industrial water	m^3	Consumption of water used for the ventilation and other cooling loads of the network EPFL1
E.I. EPFL2 Industrial water	m^3	Consumption of water used for the ventilation and other cooling loads of the network EPFL2
E.I. UNIL Industrial water	m^3	Consumption of water used for the ventilation and other cooling loads of the nearby buildings of UNIL
E.I. global Global industrial water	m^3	Cumulated consumption of water used for the ventilation and the cooling of the EPFL, UNIL and the appendixes

[1] Day index from 5 a.m. to 10 p.m. (seven days on seven), used to seperate the two different tariffs of the electricity of the day and the night

[2] Night index from 10 p.m. to 5 a.m.

LT Low temperature	MWh m^3 $°C_{departure}$ $°C_{return}$	Energetic and volumetric consumption of the LT network Supply and return temperatures of the LT network
MT Medium temperature	MWh m^3 $°C_{departure}$ $°C_{return}$	Energetic and volumetric consumption of the LT network Supply
Heat UNIL	MWh m^3	Energetic and volumetric consumption of the UNIL area
Heat EG1	MWh m^3	Energetic and volumetric production of the gas turbine 1
Heat EG2	MWh m^3	Energetic and volumetric production of the gas turbine 2.
Heat TP1&2	MWh m^3*10	Heat production of the heat pumps 1 and 2
Motor heat TP's	kWh m^3	Heat production of the heat pumps 1 and 2 by cooling of the motors of the compressors
Hours TGI	h	Running hours of the gas turbine 1
Hours TG2	h	Running hours of the gas turbine 2
Hours TP1	h	Running hours of the heat pump 1
Hours TP2	h	Running hours of the heat pump 2
Series TP1&TP2	h	Running hours of the heat pumps 1 and 2 in series
Parallel TP1&TP2	h	Running hours of the heat pumps 1 and 2 in parallel
Electricity PB1	kWh	Electricity of the pump booster 1
Electricity PB2	kWh	Electricity of the pump booster 2
Electricity PB3	kWh	Electricity of the pump booster 3
Electricity PB4	kWh	Electricity of the pump booster 4
SPP Pumping Station	kWh	Electrical consumption of the pumping station of the lake shore for both the industrial water and for the heat pumps 1& 2
Atmospheric temperature	°C	Atmospheric temperature on the EPFL site

The flowmeters are magnetic sensors. They have a precision of around ±2kg/s. The oil massmeters are Coriolis sensors. These meters have a precision of around ±2%. The energetic production is calculated by the combination of the flowmeter and of two temperature sensors (PT100, precision: ±0.05°C). The error from the electrical meter is ±1.5 % exists. The running hours sensors are digital meters. They have a precision of ±2%. The flow meters are recalibrated each year. The present tests show an error that should be a little bit bigger than the one indicates by the constructor. This additional imprecision is due to the age of these sensors (more than 11 years with a technology of 16 years). These meters will be changed in two years time.

2.2 The heating network

The buildings to be heated have a floor area of about 280000 m^2, continuously increasing as new buildings are added. These buildings are heated by two different networks:

- A medium temperature network (MT) with temperatures between 28°C and 65°C. This network was primarily designed to supply some of the older buildings (built before the decision was made to build a heat pump plant), but some of the new buildings constructed in the area of the older sites are also supplied with the medium temperature network. The buildings supplied by the MT network represent a surface of 187 000 m^2.
- A low temperature district network (LT) with temperatures between 26°C and 52°C supplies the more recent buildings. The buildings on the LT network represent a surface of 93 000 m^2.

To improve the heating performances when working with the heat pumps, the network water is delivered directly to the building radiators without intermediate exchangers. The temperatures of the networks are regulated with respect to the outside temperature (Figure 2). The district heating network is regulated with valves that are closed when the buildings have reached their temperature.

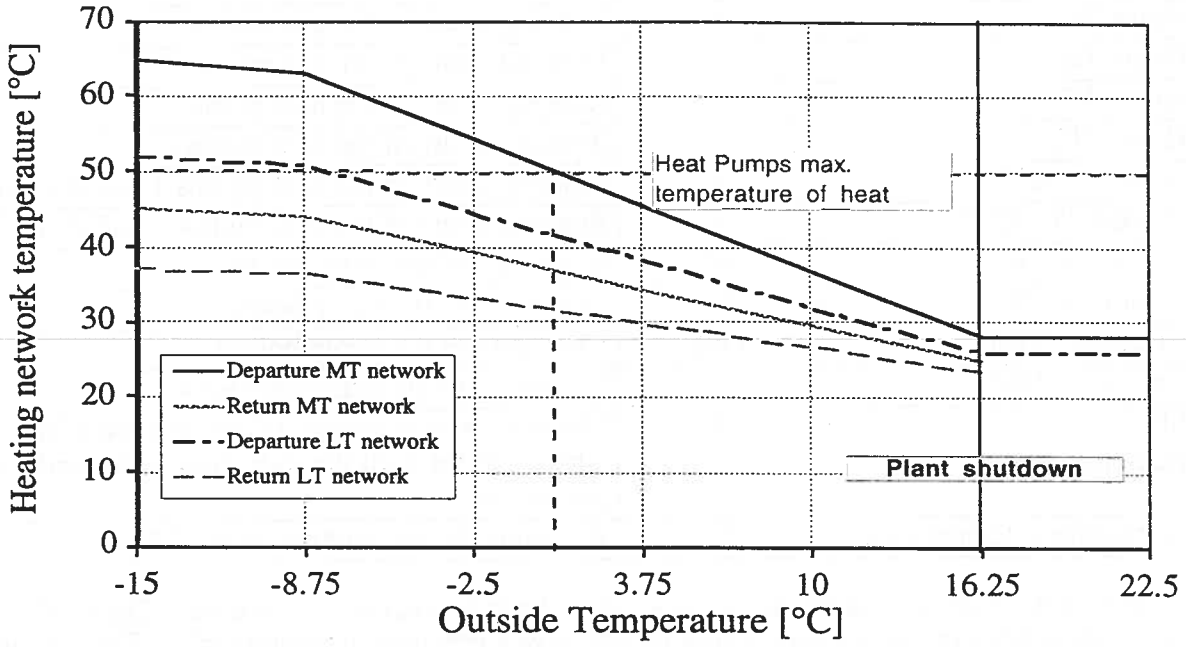

Figure 2: Network temperature regulation curves.

In the plant itself there are two flow arrangements:

- A high temperature circuit (HC) supplied by the gas turbines (max. 120°C) and connected to two of the heat storage tanks (of 110 m^3 each).
- A low temperature circuit (LC) supplied by the heat pumps with one heat storage tank of 110 m^3 (max. 52°C).

The amount of energy accumulated in the three heat tanks storage changes with the outside temperature. Lower outside temperature implies higher amounts of the energy stored. These accumulators are able to cover the daily peaks, and to equilibrate the thermal power delivered by the heat pumps and the gas turbines with the demand.

The low temperature district network is supplied by the return of the medium temperature district network with partial mixing of high temperature plant circuit water if needed.

2.3 Production

Production and consumption in Figures 3 to 11 will be often compared to the representative degree hours of the EPFL site, defined by [4]:

$$\text{Degrees hours} = \int (T_{18°C} - T_{ext})\,dh \quad \text{where if } (T_{18°C}-T_{ext}) < 0 \quad \int (T_{18°C} - T_{ext})\,dh = 0 \qquad (1)$$

Figures 3 to 9 show, as expected, that the heat production follows the curve of the degree hours except for the Christmas vacation period when the room temperatures are allowed to drop to 16°C (24th December 1996 to the 6th January 1997).

The different productions of the plant are:

- Electrical production of the gas turbines
- Heating production by the heat pumps
- Heating production by the gas turbines heat recovery unit
- Industrial water from the pumping station on the shore of the lake to the buildings.

Figure 3 shows the importance of each one of these productions (except industrial water).

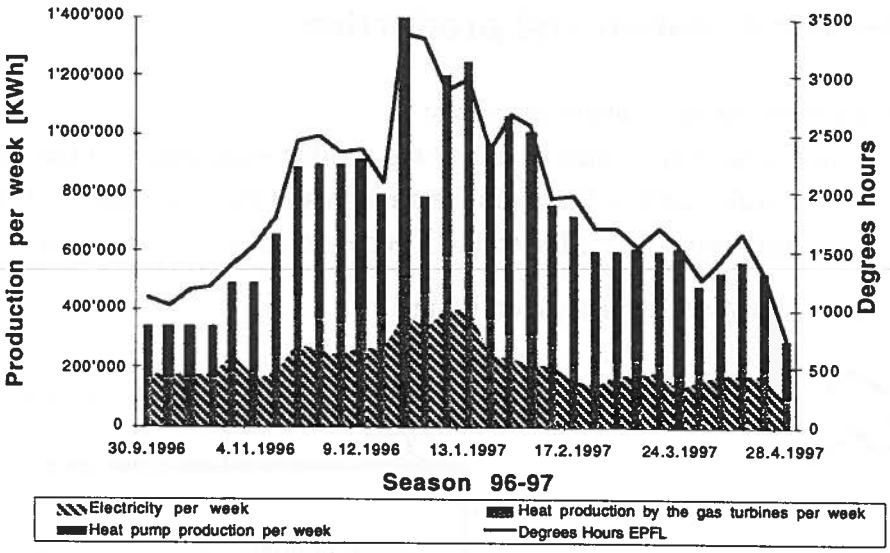

Figure 3: Productions of heat and electricity of the plant

2.4 Consumption

The different consumptions are:

- Electricity for the compressors of the heat pumps
- Electricity for the other components, pumps, light, computers...
- Heating oil for the gas turbines
- Water for the evaporators of the heat pumps

Figure 4 shows the importance of the consumption of heating oil refered to the lower heating value. The electrical consumption for light, power and other apparatus can be neglected.

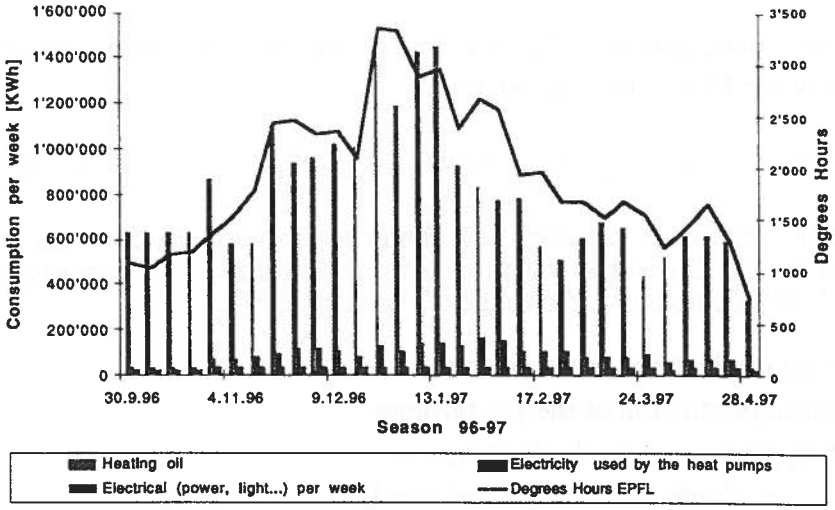

Figure 4: Electrical and heating oil consumption of the plant itself

2.5 Water consumption and production

The plant supplies different water networks:

- The industrial water, used to satisfy the cooling equipments of the laboratories
- The lake water used to warm up the ammonia in the evaporators of the heat pumps
- The heating water of the LT and MT networks, that are in a closed loop

These different networks are shown on Figure 5.

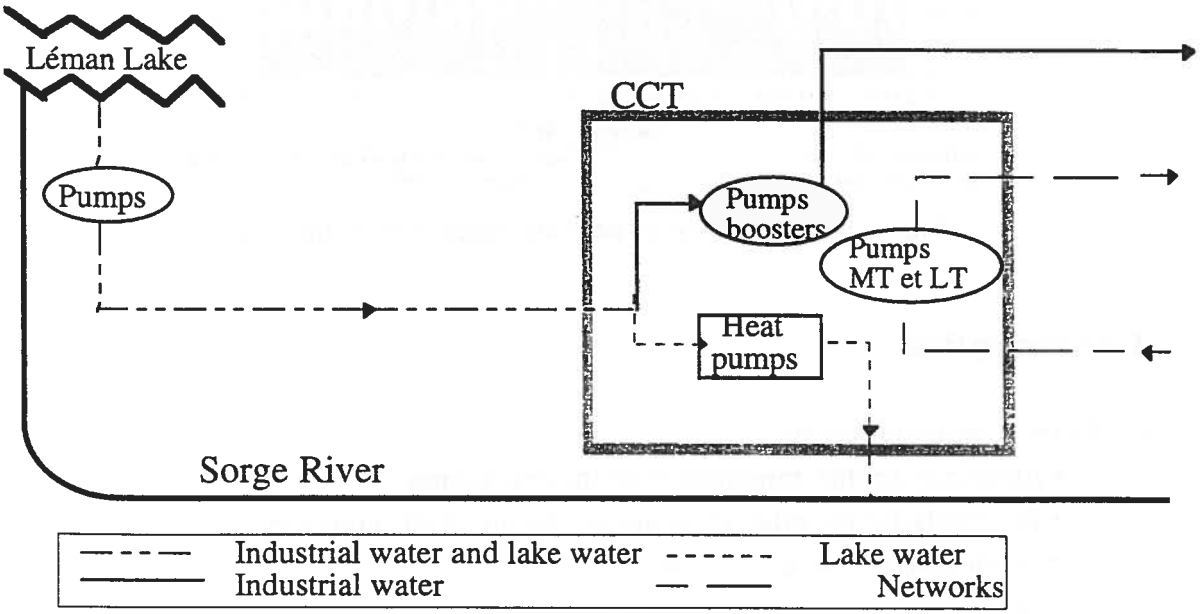

Figure 5: Sketch of the water distribution

The different consumptions and productions of the water are shown on Figure 6.

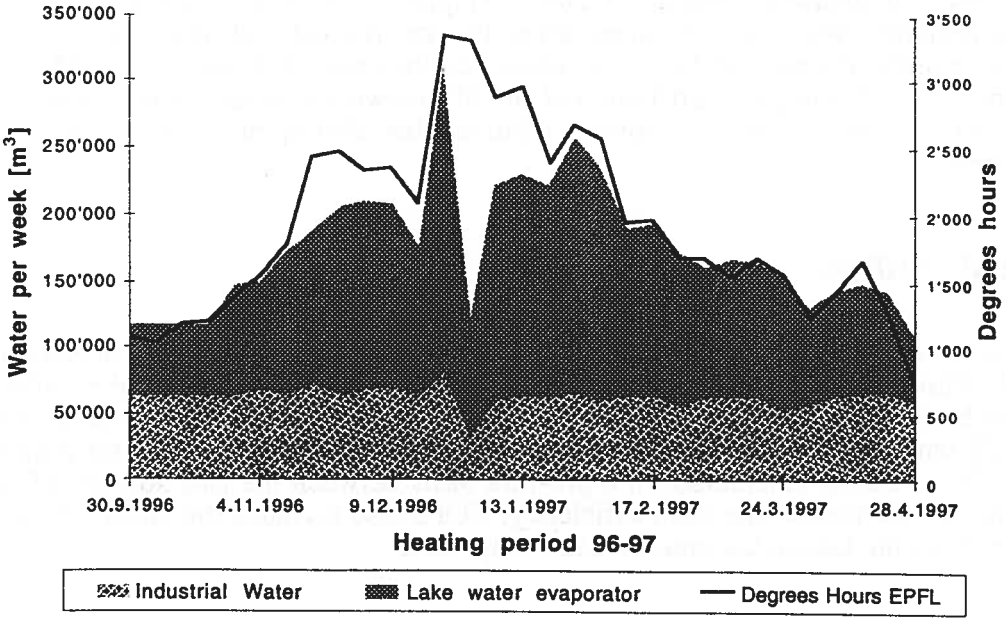

Figure 6: Consumption and production of water

This figure shows that the production of the industrial water is almost constant and does not depend on the exterior temperature. It becomes lower just during the winter holidays. An other notice is the very high consumption of water for the heat pumps. A lake or a large river are essential for such kind of large heating plants.

2.6 Heat production

Figure 7 shows the distribution of the heat supply between the gas turbines and the heat pumps and Figure 8 shows the contribution of each district heating network.

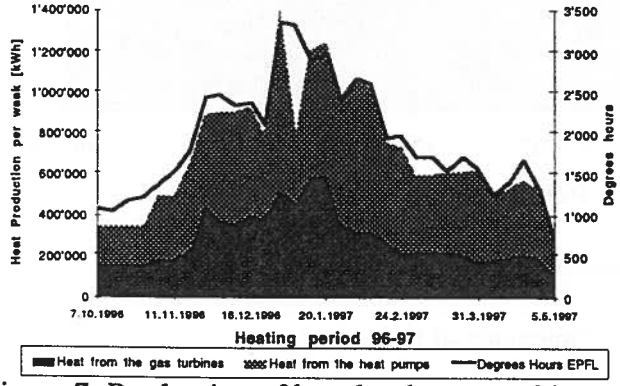

Figure 7: Production of heat by the gas turbines and the heat pumps.

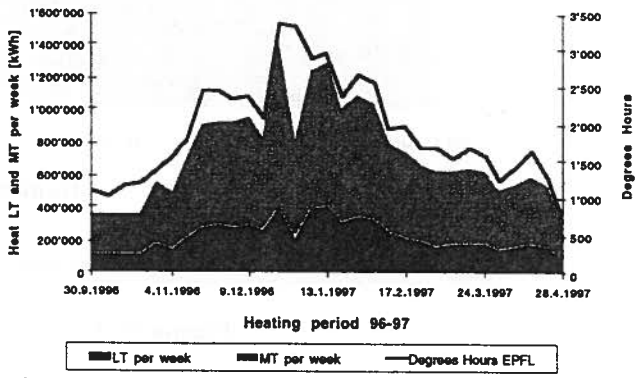

Figure 8: Distribution of heat between the LT and MT nworks.

The network temperature regulation curves (Figure 2) indicate a difference between supply and return temperatures which is 1.3 times larger for the MT network than the LT network. Figure 8 shows that in spite of a ratio of floor area heated on the order of 2, the ratio of MT/LT heat supply is on the order of 3. This larger contribution of the MT network implies a greater use of the gas turbines relative to the heat pumps, which implies a relatively bad sharing of the heat supply from an exergetic point of view.

2.7 Heat pumps

The measured efficiency of the heat pumps during the heating period under investigation is shown in Figure 9. Three different first law efficiencies are calculated. The higher efficiency COP1 is calculated by dividing the heat supplied by the electricity used by the heat pumps themselves. The second efficiency, COP2, includes in addition the electrical energy needed for pumping water in the MT and LT networks, calculated on a pro-rata basis between the two sources of heat supply (heat pumps and gas turbines). The third efficiency, COP3 also includes the energy required to pump the lake water from the lake to the creek via the evaporator.

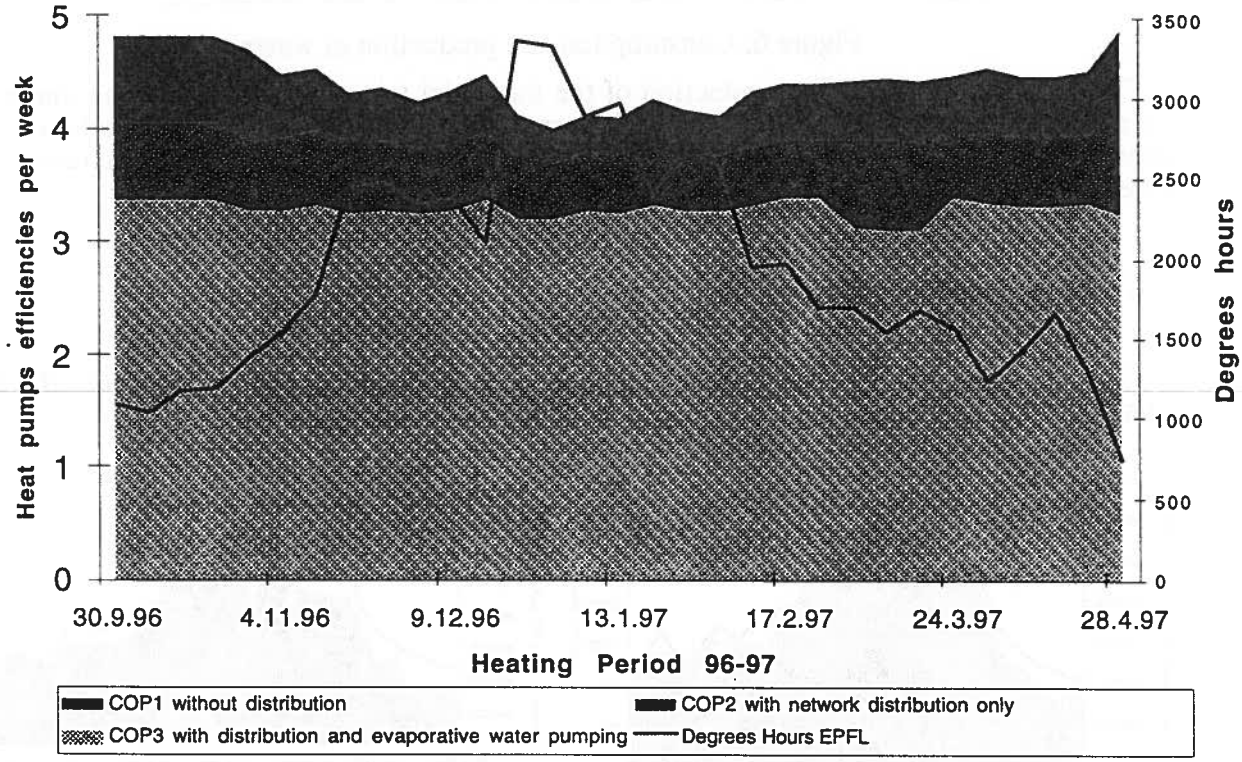

Figure 9: First law efficiencies of the heat pumps.

The different modes of use of the heat pumps are shown in the Figure 10 with the hours of running in these modes. The manner of production of the heat pumps depends on the temperature. If the difference of temperature is greater than eight (under 0°C for the outside temperature) between the return and the supply, the heat pumps will run in series. In the other conditions the system will run in parallel or alone according to the network demand.

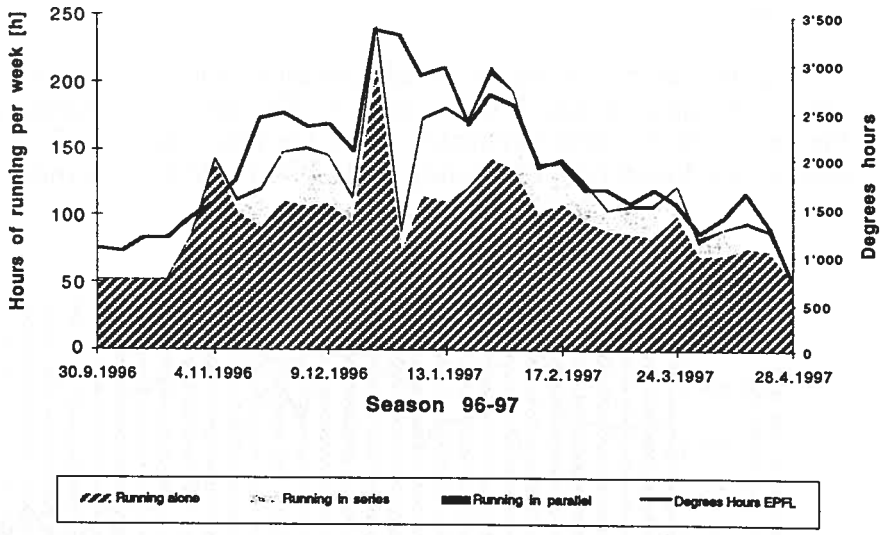

Figure 10: Type of production of the heat pumps in hours

In this graph it is surprising to see the low use of the heat pumps in parallel. It seems that it is constant during all the heating period and it does not depend on the outside temperature.

2.8 Gas turbines

It was initially planned to use the gas turbines mainly for peak shaving, as well as to heat the storage buffer tanks to boost the water temperatures of the networks, when the outer temperature drops below 0°C. However recent increases in the daily electrical utility rates and the extension of the construction surface increases the demand on the turbines. For the last heating season on which this study is based, economic considerations induced an electrically driven management of the plant, one of the gas turbines working every day from 6:30 a.m. to 6 p.m., except Saturday, Sunday and public holidays. However, the power of each gas turbine had to be reduced to 2.7 MWel since December due to problems with regulation when operating at rated power. This reduction of power induced a similar reduction of the heat supply from the gas turbine to 4.6 MWth. The second turbine was switched on when the thermal demand was too high for the combined supply of the two heat pumps and a single gas turbine, or to cut peaks in electrical demand. The other turbine is also switched on when one of the two compressors of the mechanical department is used. These compressors require 2.5 MW of electrical power.

During the day it is the electrical production that prevails over the thermal production. During the night it is the contrary. This implies that if the accumulators are full during the day and the heating network does not required anymore heat, the gas turbine will continue to run and the thermal energy that can not be stored anymore or consumed will be by-passed into the atmosphere.

This way of functioning is influenced by the way of taxing the electricity which depends on:

- The electricity consumption
- The highest electrically consuming quarter hour of the month

This last point represents approximately 50% of the EPFL's electricity bill and the running of the turbines during the day allows to cut the electrical peaks.

The size of the accumulators was not entirely sufficient to deal with this daily management regime and they were full most of the days so that frequently some of the heat had to be bypassed to the

atmosphere. During the night a turbine is switched on only if the heat pumps do not provide sufficient heat to the buildings.

During the heating period the electrical efficiency is almost constant, while the total first law efficiency varies between 53% and 73% (Figure 11). This efficiency variation is due to the use of the by-pass of the heat recovery heat exchanger when the tanks are full. To see the importance of the energy by-passed, the theoretical efficiency with 2.7/ 4.6 MW is compared to the real efficiency measured.

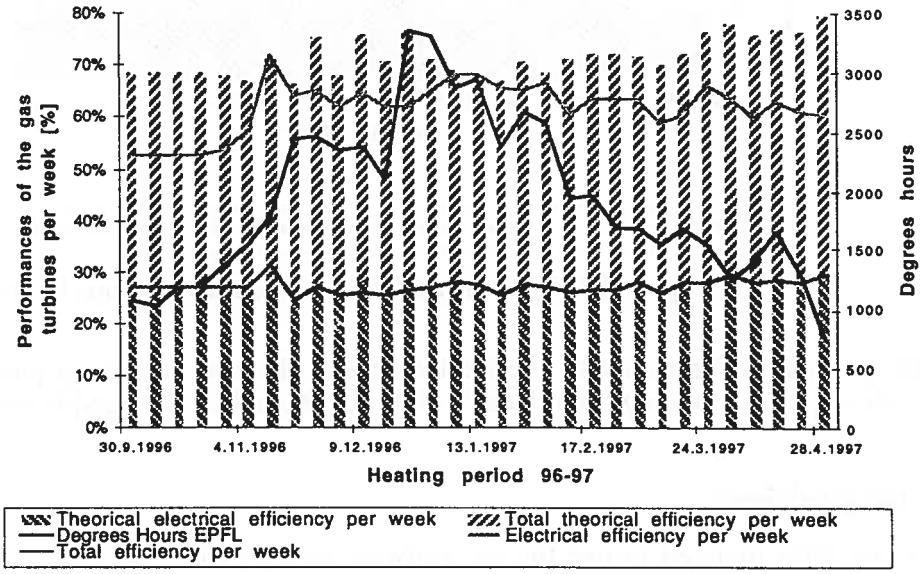

Figure 11: Theoretical versus real results.

Figure 11 shows that even when it is very cold, requiring use of the gas turbines operating at night, there is still a residual loss of thermal energy. The construction of another heat storage tank has been considered, but was rejected for different reasons:

- The investment for a new high storage tank is 2 million Frs. This sum does not include the civil engineering costs and the costs of re-equilibration of the network. 500'000 Frs must also be added for the maintenance cost every four years.
- The surface built is continuously increasing and the construction of a new accumulator will be less and less useful.
- Observations made by the personal of the plant showed that most of the time when the gas turbines produce too much energy the network does not manage to consume it during the next days then it will not be possible to consume the energy of three accumulators. And when it was very cold the gas turbines recuperators did not produce enough energy to completly fill the two heat storage tanks and therefore it is not possible to fill a supplementary accumulator.

2.9 Overall efficiency of the plant

Figure 12 shows the evolution throughout the season of the first law efficiency of the total plant, accounting or not the energy required to pump the lake water to the evaporator and the distribution of the supplied water into the networks and the buildings. As can be seen, the network and building distribution energy is not very important compared to the energy delivered.

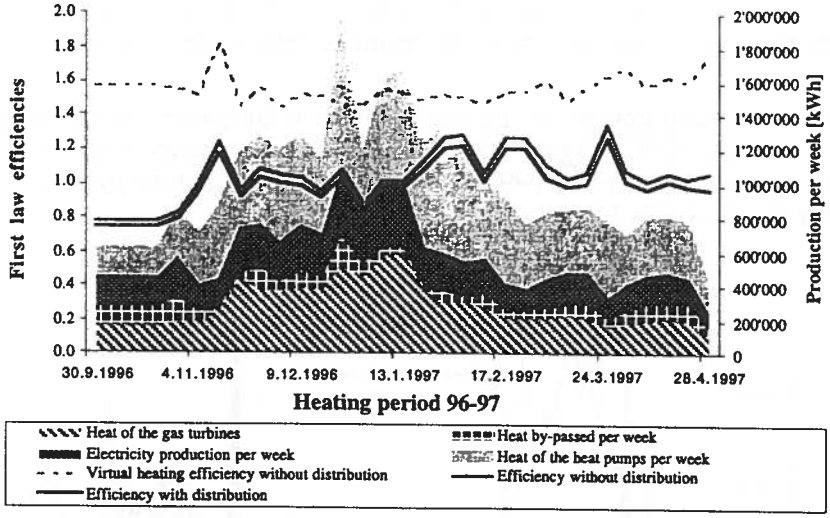

Figure 12: Efficiency of gas turbines and the heat pumps with and without distribution energy.

In terms of resource use and environmental considerations, the efficiencies are rather low considering the efficiency potential for such plants combining cogeneration and heat pumps [5]. This is unfortunately linked to the present biased economic conditions with relatively high daily electricity utility prices in Switzerland and low fossil fuel prices in the absence of any internalisation of external environmental costs. This results in a more extensive use of the gas turbines with the resulting excessive use of the bypass of the heat recovery heat exchanger. Nevertheless, if all the electricity exported from the plant was used in a heat pump having a similar COP, a virtual first law heating efficiency of the order on 160% would be obtained. The virtual first law efficiency is given by the following equation:

$$\eta_{I\,virtual} = \frac{\dot{Q}^{-}_{TG} + \dot{Q}^{-}_{HP} + (\dot{E}^{-}_{El\,prod\,TG} - \dot{E}^{+}_{El\,cons\,HP})\,COP1_{HP}}{\dot{M}_{heating\,oil}\,\Delta h_{oi}} \qquad (2)$$

As opposed to standard first law efficiencies, this virtual efficiency allows one to take proper account of the higher relative quality of electrical energy compared to heat (another approach is to use the exergetic efficiency). Without heat bypass this virtual heating efficiency could be on the order of 170%.

The following additional conclusions can be made on the basis of the 1996-1997 test period:

- Heat storage tanks are efficient only if they can be charged and discharged within frequent periods. A short calculation shows that each tank requires 38'000 kWh of excess of energy per week (on top of what is directly used for heating) to be fully charged. With the present strategy, this condition would be fulfilled twenty-seven weeks out of thirty-two, and the conditions are always met to entirely discharge the tank every week. Real observations do not fully confirm this and attention should be given to improving the management of the storage tanks, possibly through the introduction of predicted management schemes [6].
- An integration of the electrical consumption of the EPFL could also be envisaged in the regulation system of the gas turbines.
- The demand ratio between the medium and low temperature networks is unfavourable to an optimum use of the heat pumps which are presently limited to 50°C.
- The correction of the gas turbine regulation problem to operate again at the rated conditions (3/6 MW) will further increase the need for gas by-passing and the option of a new high temperature storage tank should be reconsidered. However the future liberalisation of the electricity market might

induce a significant lowering of the daily rates to medium size electricity users like the EPFL and therefore open the way to new and more environmentally positive strategies.

• Actually the thermal energy of the gas turbines is by-passed in the atmosphere when the outside temperature is around 12°C (Figure 13). This figure also shows that the regulation system could be improve (for example March 18 1997 at 10 am a supplementary turbine was switched on and just a few hours later the heat was by-passed).

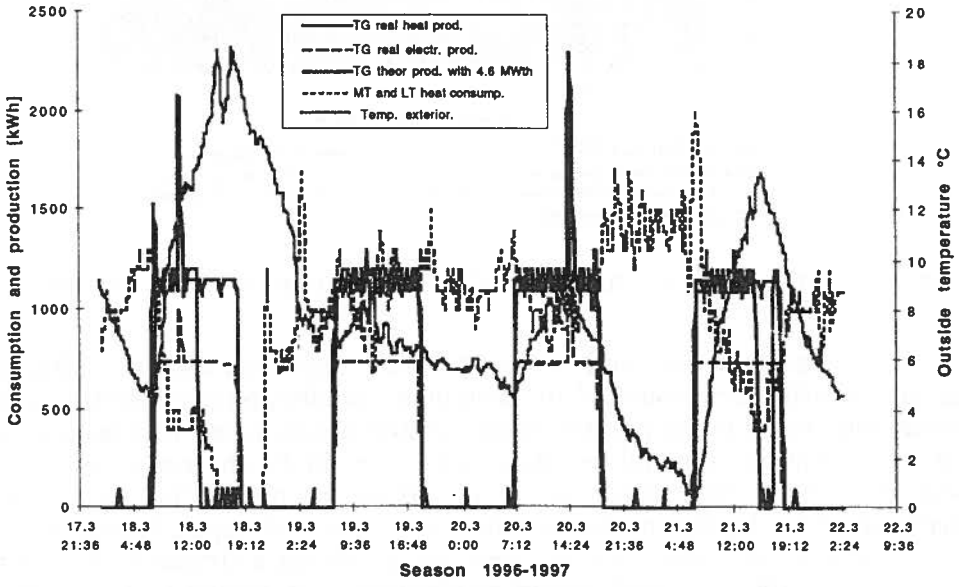

Figure 13: Analyse of the production of the gas turbines during four days

It is significant to note that a new optimisation of the plant was introduced at the end of the heating season 1996-1997. Figure 14 shows this amelioration. If we compare the beginning and the end of the heating season we notice a significant decrease of the thermal energy by-passed.

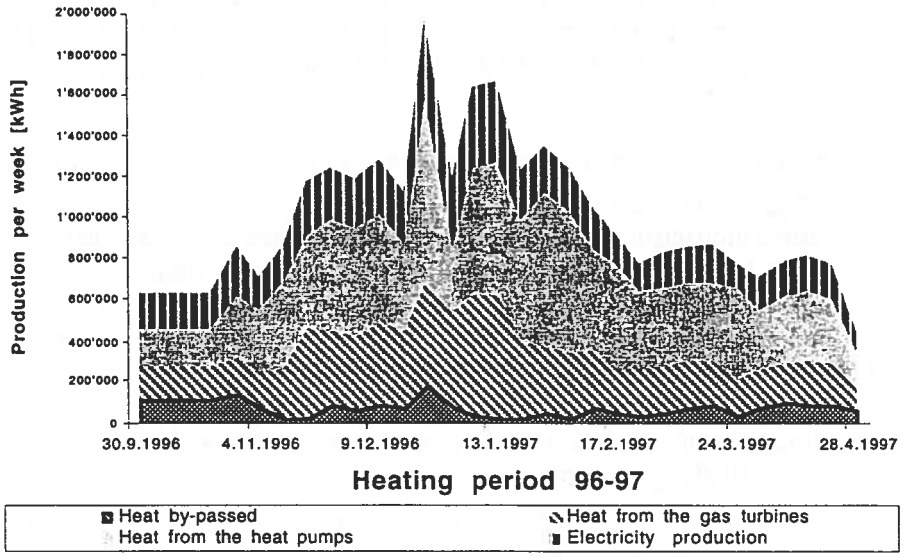

Figure 14: Analysis of the thermal production

3. DETAILED ANALYSIS OF HEAT PUMP N°2

One of the main objectives of this study is to monitor the performance of the two ammonia heat pumps after eleven years of operation and compare this data with earlier data, particularly those measured by the supplier during the commissioning period. Both heat pumps have a similar cumulated time of operation (21600 hours in March 1997 for heat pump No 2), and only the latter is completely instrumented. All tests of the last heating period are made with the economizer port connected. The earlier tests of the supplier included cases with and without the economizer.

3.1 Ammonia cycle

The ammonia vapour coming from the evaporator is compressed by an oil injected twin screw compressor. As usual for this type of machine, the oil mass flow is more than three times higher than the refrigerant mass flow which requires a large oil separator at the discharge of the compressor to reduce the amount of oil entrained to the condenser. The refrigerant and the remaining oil flow through a subcooler, to the first expansion valve, and into the economizer vessel. The separated vapour flows back to the economizer port of the compressor while the remaining liquid undergoes a second expansion to the spray type of shell and tube evaporator. The remaining oil tends to build up in the accumulator at the bottom of the evaporator and oil draining is done automatically at each start up of the heat pump. If the economizer port is not used, the refrigerant is bypassed after the first expansion valve, which then ensures a full expansion. The lake water circulates inside the tubes of the evaporator in a four pass arrangement. (Figure 15).

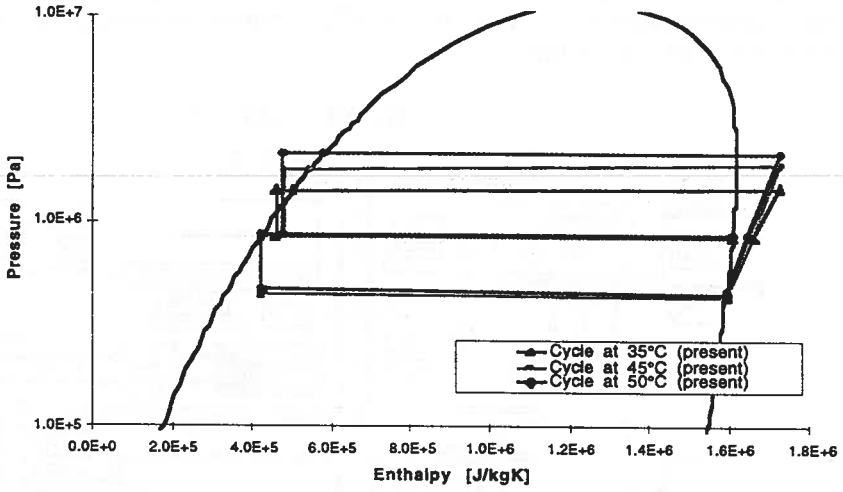

Figure 15: Present cycles at different supply temperatures

The heating network water is heated successively through the subcooler, the oil cooler and the condenser. A secondary fluid stream recovers the thermal losses of the electric motor. Figure 16 shows the importance of the heat coming from these different elements.

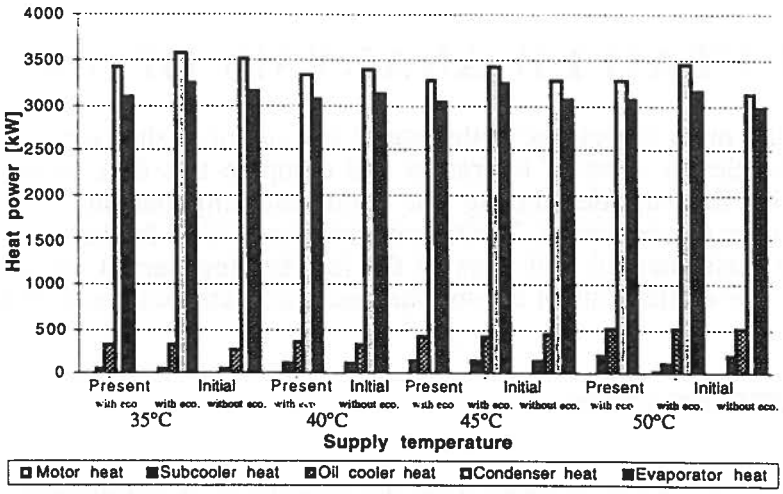

Figure 16: Supply heat power

The heat pumps are regulated by controlling the supply water flow and the expansion valve at the exit of the subcooler. A supplementary regulation system is used when the heat pumps reach the limit of running (upper 50°C) to allow them to continue to work.

3.2 Measurements

The refrigerant, water and oil circuits of the second heat pump are fully instrumented. An analysis of the major components of the heat pump n°2 is based on conditions when only the heat pump n°2 was workingin stable conditions.

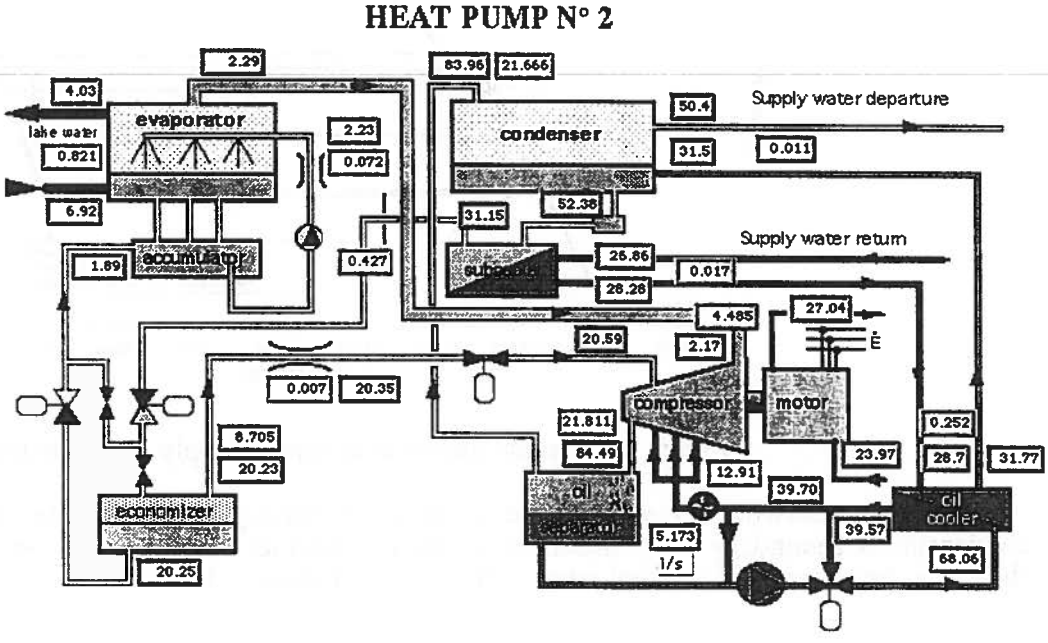

Figure 17: Typical screen dump from the data acquisition computer.

The data from the transducers are collected in a computer equipped with the software Lab View. This computerised data acquisition is completely separated from the operational measurements, and

from the control room computer. Such additional equipment allows a regular and accurate check of performances. It provides data for validation of models and facilitates students' experiments without disturbing the operation of the plant.

Comparison will be showed between tests made by LENI and previous tests made by Sulzer. It is important to note that the Sulzer measurements are not all based on the same transducers. The temperatures sensors in particular are not the same and are not situated exactly at the same place. Some pressure sensors are identical with those used by LENI, but the majority of them are located at different places. There are also sensors that are unique to either LENI or Sulzer measurements.

A list of the captors is shown in the Table 2 and the

Table 3 with an indication if they are measured by LENI or/and Sulzer.

Table 2: List of the pressure sensors

	Pressure	Sensors	LENI	Sulzer	Precision
500	Entry NH3 compressor	Absolu pressure	x	x	±0.05 bar
501	Exit NH3 compressor	Absolu pressure	x	x	±0.05 bar
502	Entry condenseur	Absolu pressure	x	x	±0.05 bar
503	ΔP diaph.debit condenser NH3	Differential pressure	x	x	±0.05 bar
504	ΔP vent.debit accumumulator NH3	Differential pressure	x	x	±0.05 bar
505	Exit NH3 evaporator	Absolu pressure	x	x	±0.05 bar
506	Venturi economizer NH3	Absolu pressure	x	x	±0.05 bar
507	ΔP venturi economizer NH3	Differential pressure	x	x	±0.05 bar
508	Entry NH3 eco.compressor	Absolu pressure	x	x	±0.05 bar
509	ΔP water evaporator	Differential pressure	x		±0.05 bar
510	ΔP water subcooler.	Differential pressure	x		±0.05 bar
511	ΔP water oil cooler	Differential pressure	x		±0.05 bar
512	ΔP water condenser	Differential pressure	x		±0.05 bar
513	P entry oil compressor	Absolu pressure	x	x	±0.05 bar

Table 3: List of the temperature sensors

	Temperatures	Sensors	LENI	Sulzer	Precision
109	Entry NH3 compressor	PT 100	x	x	±0.05°C
108	Exit NH3 compressor	PT 100	x	x	±0.05°C
107	Entry NH3 condenser	PT 100	x	x	±0.05°C
106	Entry NH3 subcooler	PT 100	x	x	±0.05°C
105	Exit NH3 subcooler	PT 100	x	x	±0.05°C
104	Exit NH3 liquid economizer	PT 100	x	x	±0.05°C
103	Entry NH3 accumulator	PT 100	x		±0.05°C
102	Venturi accumulator NH3	PT 100	x		±0.05°C
101	Exit evaporator NH3	PT 100	x	x	±0.05°C
100	Exit NH3 vapor economizer	PT 100	x	x	±0.05°C
200	Venturi economizer NH3	PT 100	x		±0.05°C
201	Entry NH3 economizer.-compressor	PT 100	x	x	±0.05°C
202	Entry water evaporator	PT 100	x	x	±0.05°C
203	Exit water evaporator	PT 100	x	x	±0.05°C
204	Entry water subcooler	PT 100	x	x	±0.05°C
205	Exit water subcooler	PT 100	x		±0.05°C
206	Entry water oil cooler	PT 100	x	x	±0.05°C
207	Exit water oil cooler	PT 100	x		±0.05°C
208	Entry water condenser	PT 100	x	x	±0.05°C
209	Exit water condenser	PT 100	x	x	±0.05°C
300	Entry water motor	PT 100	x		±0.05°C
301	Exit water motor	PT 100	x		±0.05°C
302	Entry oil cooler	PT 100	x		±0.05°C
303	Exit oil cooler	PT 100	x		±0.05°C
304	Entry oil compressor	PT 100	x	x	±0.05°C
500	Oil separator	PT 100		x	±0.05°C

The values of electricity consumption and of water flows (supply water, motor, evaporator) are taken manually from the plant's meters (Table 4).

Table 4: Meters of the plant

	Meters	Sensors	LENI	Sulzer	Precision
1	Electrical meter		X	X	±0.02 kW
2	Water lake meter	Magnetic flowmeter	X	X	±2 kg/s
3	Supply water meter	Magnetic flowmeter	X	X	±2 kg/s
4	Motor water flow	Magnetic flowmeter	X	X	±2 kg/s
5	Oil flow meter	Propeller flowmeter	X	X	±1 kg/s

These measurements are treated by a Fortran program made by LENI.

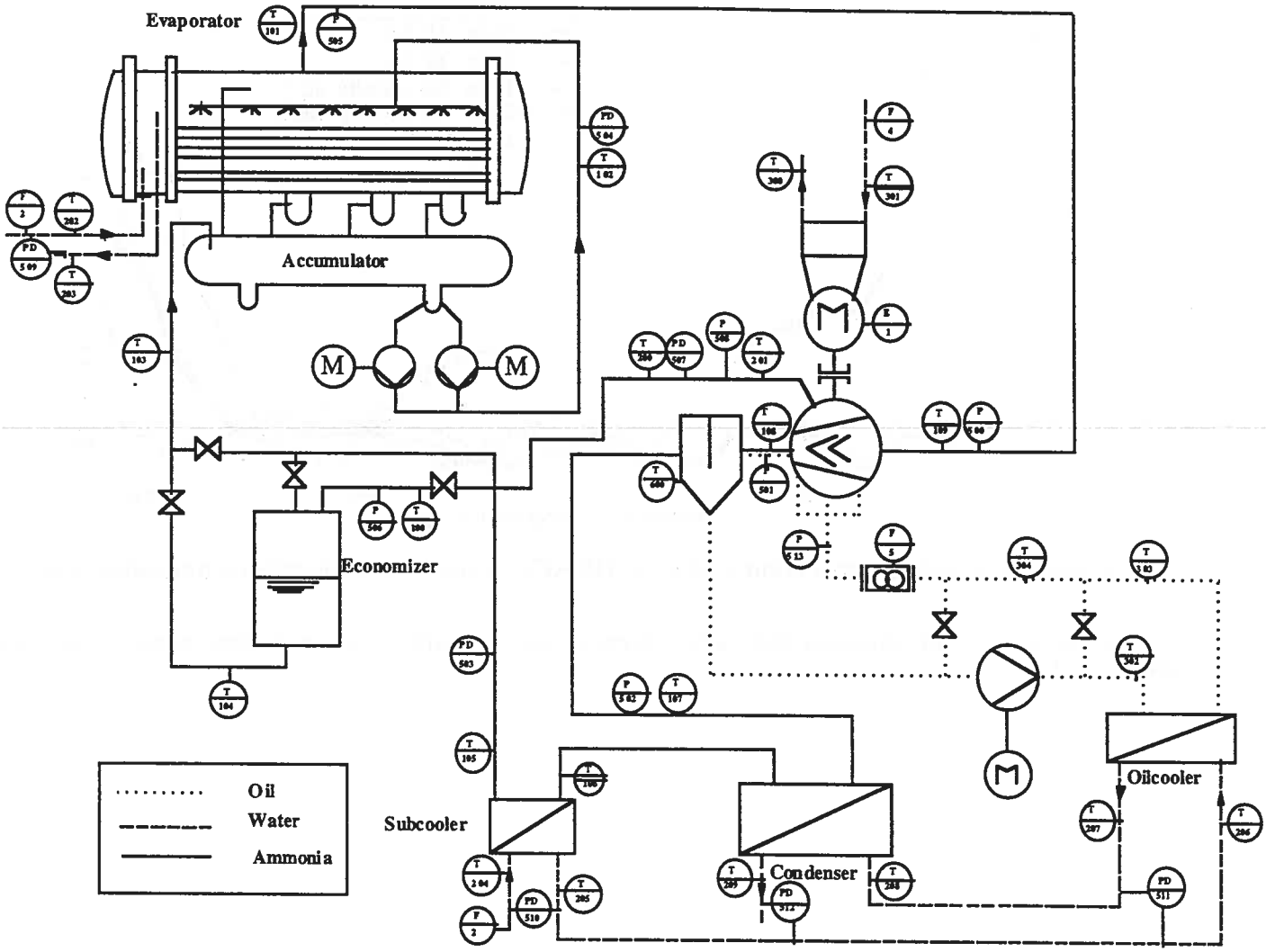

Figure 18: Captors on the heat pump n°2

3.3 Thermodynamic states

To get the different ammonia states, two programs were chosen for comparison. The first one is based on the equations of Lee Kesler and the second one based on the equations of Reynolds. Some comparative trials with the values given by ASHRAE [7] indicate that the equations of Reynolds were much more precise than the result given by Lee Kesler. The precision of Reynolds equations is very high as can be seen on the two following graphs. The first one gives the error on the saturated pressure, density, enthalpy, and the entropy compared to ASHRAE's values when the saturated temperature is given (Figure 19) .

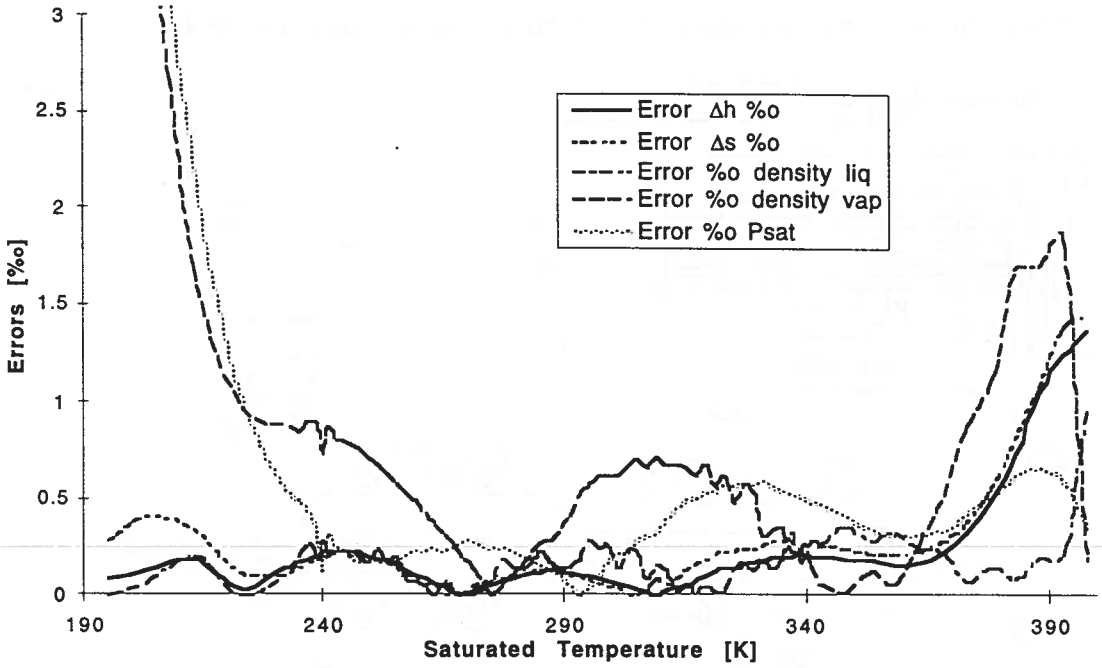

Figure 19: Relative errors compared to ASHRAE's values with a saturated temperature given.

The second graph provides the same thermodynamic states when saturated pressure is given (Figure 20).

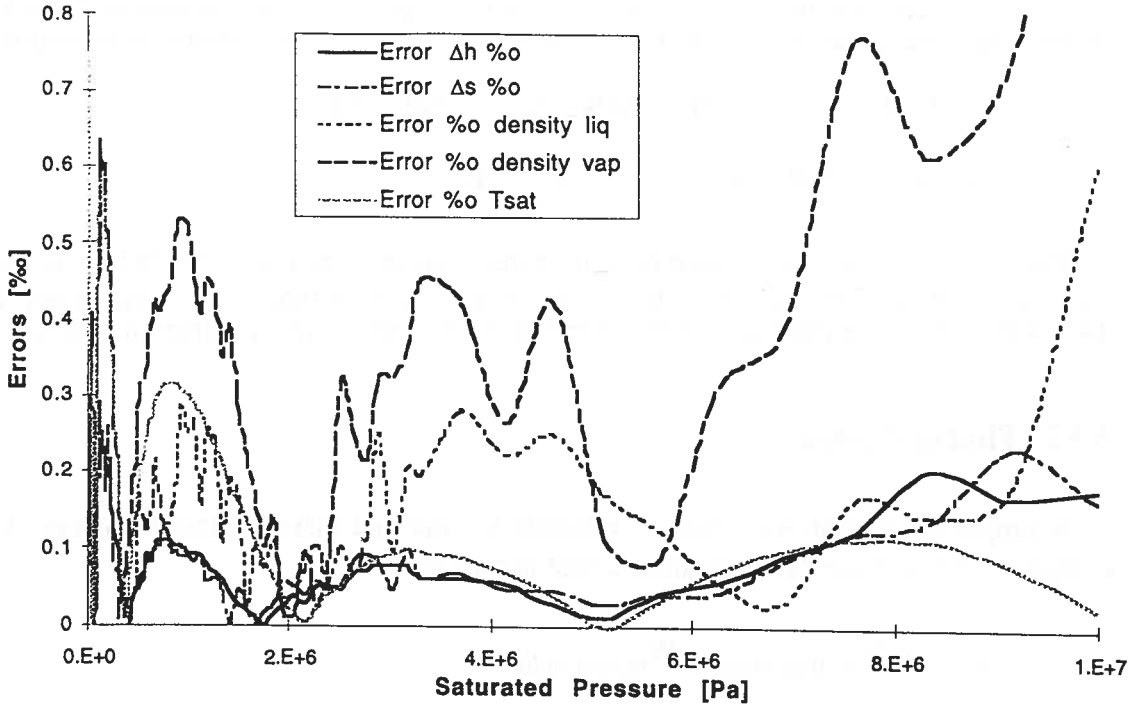

Figure 20: Relative error compared to ASHRAE's values with a saturated pressure given.

Sulzer for its calculation uses two other programs, one for the refrigerant called KMST, the other for the water called FLST. These two programs were developed by Sulzer.

In appendix I the different methods for calculating various elements of the heat pump. are compared and explained in more detail

3.3.1 Calculation on the water and oil

Due to the small variations on the pressure and temperature of the water and of the oil, the calculation of the thermodynamic states is made by the following approximations:

$$du \cong Cp\, dT \qquad (3)$$

$$dh \cong Cp\, dT + vdP \qquad (4)$$

$$ds \cong \frac{Cp}{T} dT \qquad (5)$$

NB: If the pressure P is not known, the pressure-drop (P_{out}-P_{in}) is neglected.

Values used for the calculation

Cp_{H_2O} = 4.187 [KJ/kg.°C]

ρ_{H_2O} = 999.48 [kg/m^3]

For the oil, the specific heat and the volumetric mass have been measured by taking a sample of the oil which was analysed by a external laboratory. It gives the following relationship:

$Cp_{oil}(T) = 0.332\ 10^{-2}\ T + 1.887$ [KJ/kg.°C] with T [°C]

$\rho_{oil}(T) = 1060\text{-}0.2572\ T$ [kg/m^3] with T [°K]

British Petroleum, the oil supplier, indicates a specific heat of 1.95 [kJ/kg K] and a volumetric mass of 0.994 [8]. The difference is due to the ammonia included in the oil, which the oil separator did not manage to separate completely because there is still some quantity in solution.

3.3.2 Thermal losses

A simple calculation was made to estimate the thermal losses in the exchanger $\dot{Q}^{-}_{loss}$ in order to compare them to those calculate from a first law balance.

$$\dot{Q}^{-}_{loss} = \dot{W}^{+}_{heating\ fluid} - \dot{W}^{-}_{heated\ fluid} \qquad (6)$$

Where $\dot{W}^{+}$ is the enthalpy difference.

This estimation was made by calculating the heat transfer loss between the shell of the exchanger and the ambient air.

The heat resistance on the fluid side (inside the exchanger) can be neglected compared to the other thermal resistance. There is two resistance left, one of conductance and an other of convection outside the exchanger.

The conductance resistance is:

$$R_{th\ cond} = \frac{Thickness}{\lambda\ .\ A_{middle}} \quad [°K/W] \qquad (7)$$

with $A_{middle} = \Pi\ \bar{d}\ L.$ [m^2]

$\lambda_{steal} = 60.5$ [W/(m.K)]

The convection resistance has been calculated using the Churchill and Chu relation, describing the external free convection around a cylinder [9].

This relation is applicable for a large Rayleigh range: $10^{-5} < Ra < 10^{-2}$

$$Nu_d = \left\{ 0.6 + \frac{0.387\ Ra_d^{1/6}}{\left[1 + (0.559/Pr)^{9/16}\right]^{8/27}} \right\}^2 \qquad (8)$$

$$\text{with } Ra = \frac{d^3 g \beta (T_{surface} - T_{fluid})}{\nu^2} Pr \qquad (9)$$

The physical properties of the air are considered at the average temperatures between the temperature of the surface and of the room:

$$T_{fluid} = \frac{T_{ext} + T_{surfae}}{2}$$

The volumetric thermal expansion coefficient is calculated with the hypothesis of a perfect gas:

$$\beta = \frac{1}{T_{fluid}} [°K^{-1}] \qquad (10)$$

Then the heat rate becomes:

$$\alpha_{air} = \frac{Nu_d \lambda_{air}}{d} \qquad (11)$$

$$R_{th\ conv\ air} = \frac{1}{\alpha_{air} . A} \qquad (12)$$

$$\dot{Q}_{conv+cond} = \frac{\Delta T_{log}}{R_{th\ cond} + R_{th\ conv_{air}}} \qquad (13)$$

The influence of the radiation is taken in account with the Stefan-Boltzmann law:

$$\dot{Q}_{rad} = A \varepsilon \sigma (T_{surface}^4 - T_{ext}^4) \qquad (14)$$

With the Boltzmann's constant $\sigma = 5.67\ 10^{-8}$ [W/m²K⁴]

and the emissivity of the grey paint ε=0.9

The sum of the two heat power gives an estimation of the exchanger loss:

$$\dot{Q}_{loss} = \dot{Q}_{rad} + \dot{Q}_{conv+cond} \qquad (15)$$

3.4 Total efficiency

According to the first law applied to the heat pump [10]:

$$\dot{E}_{El}^{+} + \dot{W}_{H_2O\ Ev}^{+} = \dot{W}_{H_2O\ Supply}^{-} + \dot{Q}_{Loss}^{-} \qquad (16)$$

$\dot{E}_{El}^{+}$: the electrical power takes into account:

- the power for the motor of the compressor,
- the power for the oil pumps (7 kW)
- the power for the ammonia pumps at the exit of the accumulator (9 kW)

$\dot{W}^{-}_{H_2O\ Supply}$: the enthalpy difference for the supply water takes into account the heat from:

- the subcooler
- the condenser
- the oil cooler
- the motor cooler

The second law balance is:

$$\dot{E}^{+}_{e_{El}} + \dot{E}^{+}_{W_{H_2O\ Ev}} = \dot{E}^{-}_{W_{H_2O\ Supply}} + \dot{L} \qquad (17)$$

Where $\dot{E}_W$ is the difference of coenthalpy (mass flow exergies) in the networks considered.

Last year's results, during the eleventh year of operation, indicate a non negligible decrease in efficiency (Figures 21 and 22) at all operating conditions. Recent measurements in a configuration with an active economizer are compared to two sets of earlier results (with and without an active economizer). It is note worthy that for the same delivery temperature, the mass flowrate can vary depending upon the return temperature of the water. This explains why the equivalent first law efficiencies (COP) do not translate into equivalent second law efficiency values as can be seen when comparing Figure 21 and 22.

The efficiencies of the heat pump are: $\eta_I = \dfrac{\dot{W}^{-}_{H_2O\ sup\ ply}}{\dot{E}^{+}_{El}}$ $\eta_{II} = \dfrac{\dot{E}^{-}_{W_{H_2O\ Supply}}}{\dot{E}^{+}_{e_{El}}}$ (18)

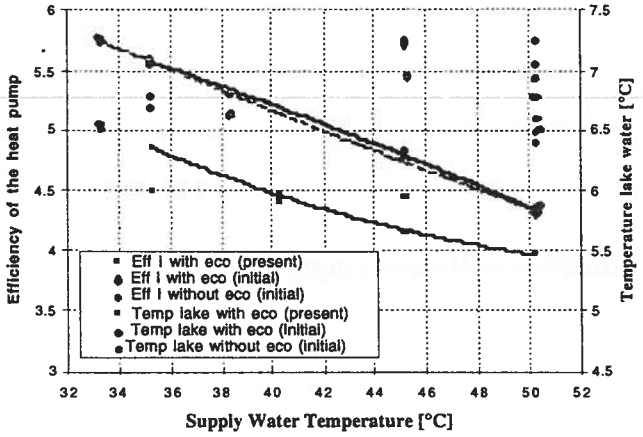

Figure 21: Efficiency of the heat pump.

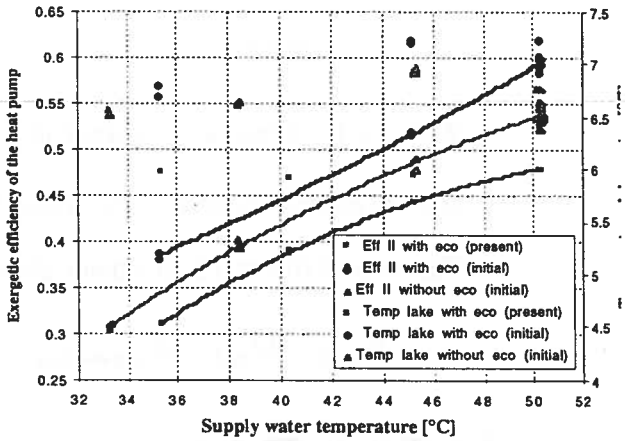

Figure 22: Exergetic efficiency of the heat pump.

For operational reasons and to avoid disturbances to occupant comfort, some of the tests had to be made over weekends with an "artificial" control of the supply with, for example, a lowering of the mass flow rate. In these conditions pinch temperature can be influenced. Therefore exergetic efficiencies are the best measure for comparison.

The reasons for the lower efficiency seems to be a lowering of the compressor efficiency. Most of the other component performances compare well with the initial test results. Fouling of the evaporator, although not very significant, also contributes to the performance reduction as can be seen from the temperature profiles. In addition the presence of some inert gases during the present tests might alow be a cause of degradation. Efficiency comparisons for the major components are shown below.

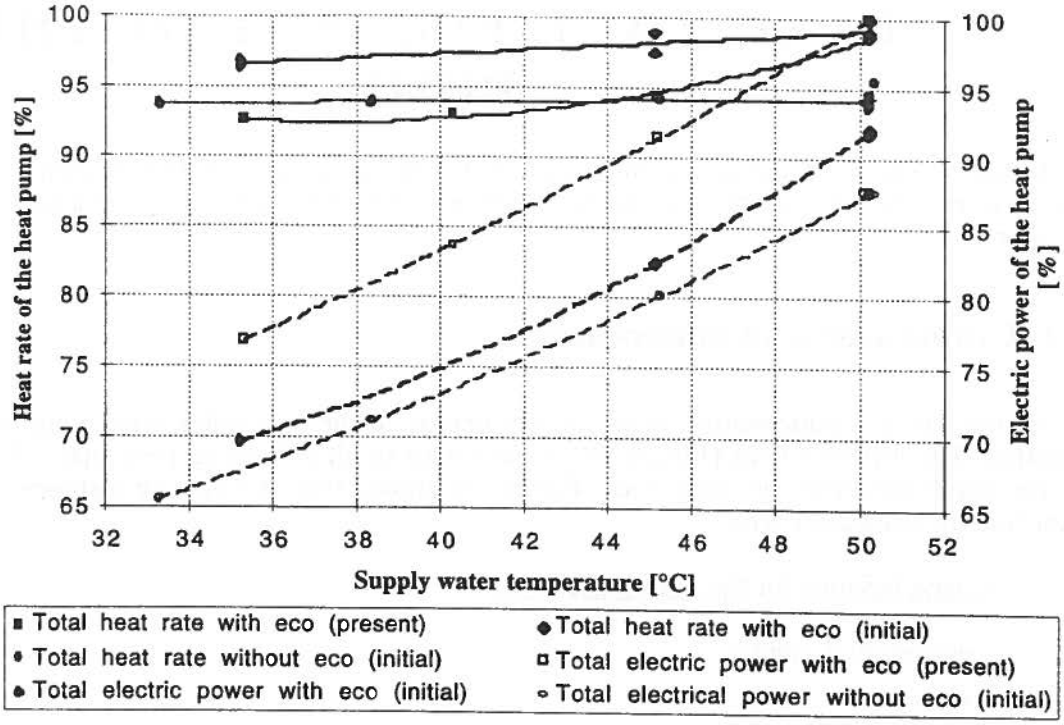

Figure 23: Tendency of evolution of the heat rate delivered and of the electricity consumed by the heat pump.

4. STUDY OF EACH ELEMENT OF THE HEAT PUMP

To know exactly what is the difference between initial and present results, and to see as well which improvement can be done to each element, we will study them separately in the following chapters.

4.1 Condenser and subcooler

As the end of condensation occasionally occurs in the subcooler both equipments are analysed together. The different tests (Figure 24) show a very small difference (less than 1%) on the efficiency of the condenser and the subcooler. Figure 24 shows that the energy balance is well within the expected measurement error.

Characteristics for the condenser [11]:

•External diameter	1 m
•Length	6.4 m
•Double-pass exchanger with plain carbon steel tube	
•Water fouling factor	10^{-4} m²K/W
•Ammonia fouling factor	0 m²K/W
•Water pressure-drop (constructor)	7.6 kPa
•Water pressure-drop (average calculated for the present tests)	4.7 kPa
•Thermodynamic loss (average calculated for the present tests)	8.69 kW
•Pinch temperature (average calculated for the present tests)	2.47 °C

Characteristics for the subcooler:

•External diameter	0.5 m
•Length	1 m
•Single-pass exchanger with plain carbon steel tube	
•Water fouling factor	$2*10^{-4}$ m²K/W
•Ammonia fouling factor	0 m²K/W
•Water pressure-drop (constructor)	5.5 kPa
•Water pressure-drop (average calculated for the present tests)	4.9 kPa
•Thermodynamic loss (average calculated for the present tests)	0.24 kW
•Pinch temperature (average calculated for the present tests)	2.34 °C

The thermodynamic balance according to the first law is given by the equation:

$$\dot{W}^{-}_{H_2O\,C} + \dot{W}^{-}_{H_2O\,AC} + \dot{Q}^{-}_{Loss} = \dot{W}^{+}_{NH_3\,C} + \dot{W}^{+}_{NH_3\,AC} \qquad (19)$$

According the second law gives:

$$\dot{E}^{+}_{W_{NH_3}\,AC} + \dot{E}^{+}_{W_{NH_3}\,C} = \dot{E}^{-}_{W_{H_2O}\,C} + \dot{E}^{-}_{W_{H_2O}\,AC} + \dot{L} \qquad (20)$$

The efficiencies are: $\eta_I = \dfrac{\dot{W}^{-}_{H_2O\,C} + \dot{W}^{-}_{H_2O\,SC}}{\dot{W}^{+}_{NH_3\,C} + \dot{W}^{+}_{NH_3\,SC}}$ $\eta_{II} = \dfrac{\dot{E}^{-}_{W_{H_2O}\,C} + \dot{E}^{-}_{W_{H_2O}\,SC}}{\dot{E}^{+}_{W_{NH_3}\,SC} + \dot{E}^{+}_{W_{NH_3}\,C}}$ (21)

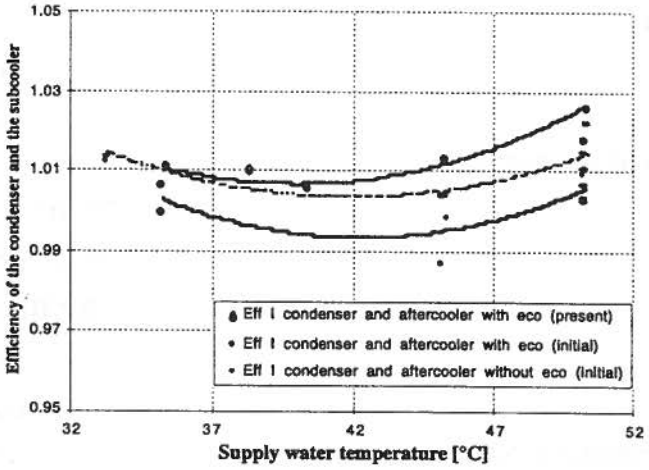

Figure 24: Efficiency of the condenser and the subcooler

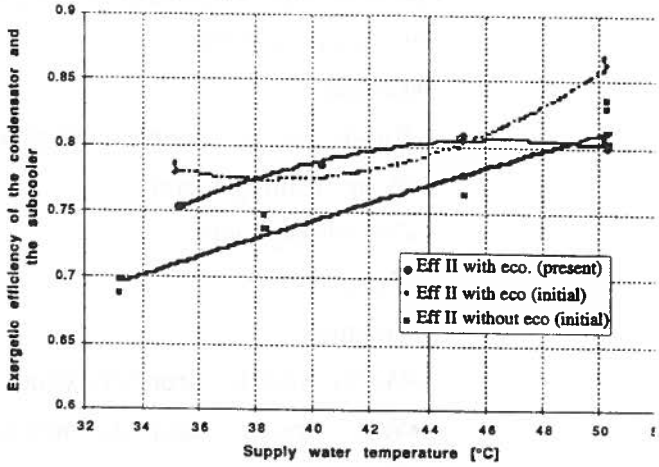

Figure 25: Exergetic efficiency of the condenser and the subcooler

Figure 26 considers the temperature difference between refrigerant and heated fluid at a location between the subcooler and the condenser. This temperature difference has been taken at this place because it is the place where the different sensors of LENI and Sulzer were closer. An augmentation of the temperature difference is noticed in the condenser and the subcooler. This augmentation can be attributed to the presence of inert gases in the condenser.

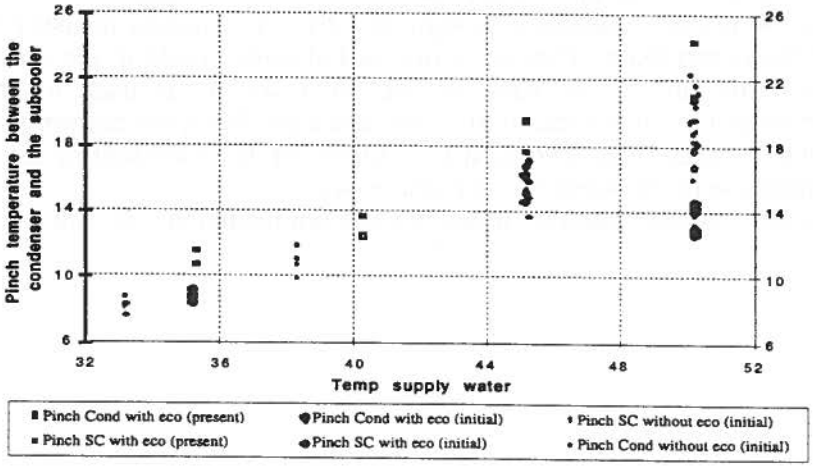

Figure 26: Temperatures differences between refrigerant and heated water at a location between the condenser and subcooler

We have however to be careful with conclusions on this point as the results of exergetic efficiency (Figure 25) do not show a clear trend between earlier and present tests.

4.2 Oil cooler

The oil cooler is used to cool down the oil coming from the compressor before reinjecting it into the compressor. The heat exchange is made with the supply water.

Only present tests are shown because there is not enough temperature sensors on the Sulzer's measurements on the oil cooler. The temperature sensors of Sulzer did not allow to calculate an efficiency on the oil cooler.

Characteristics for the oil cooler [11]:

•External diameter	0.5 m
•Length	2.5 m
•Single-pass exchanger with plain carbon steel tube	
•Water fouling factor	$2*10^{-4}$ m²K/W
•Oil fouling factor	$2*10^{-4}$ m²K/W
•Type of oil	BP Breox 75
•Quantity	800 kg
•Water pressure-drop (constructor)	10.2 kPa
•Water pressure-drop (average calculated in the present tests)	25 kPa
•Thermodynamic loss (average calculated in the present tests)	1.17 kW
•Pinch temperature (average calculated in the present tests)	9.13 °C

The oil cooler circuit for the compressor included two by-passes(Figure 27). Through the first one the oil cooled by the water is injected just before the pump and is mixed with the hot oil coming from the compressor. The second by-pass deviates a certain amount of oil away from the oil exchanger. Its entry is situated between the oil pump and the entry of the oil cooler, its exit is just after the oil cooler. This by-pass permits a regulation of the temperature between 45°C and 50°C (best viscosity of the oil). Hence the high pinch temperature of the oil exchanger.

The oil flow in the compressor is regulated by a differential pressure sensor between the oil entry and exit of the compressor. This oil is injected at three points in the compressor: at the entry, by the economizer entry and at the exit. At the entry the oil is used to lubricate the screws. At the economizer entry the oil is used to lubricate and cool down the compressor. At the exit the oil is used to cool down the ammonia. The goal is to inject the least amount of oil as possible otherwise it will lead to an increase in the work of the compressor.

The oil circuit is composed by tubes that are not insulated, only the oil separator is insulated.

The sketch of the oil circuit is:

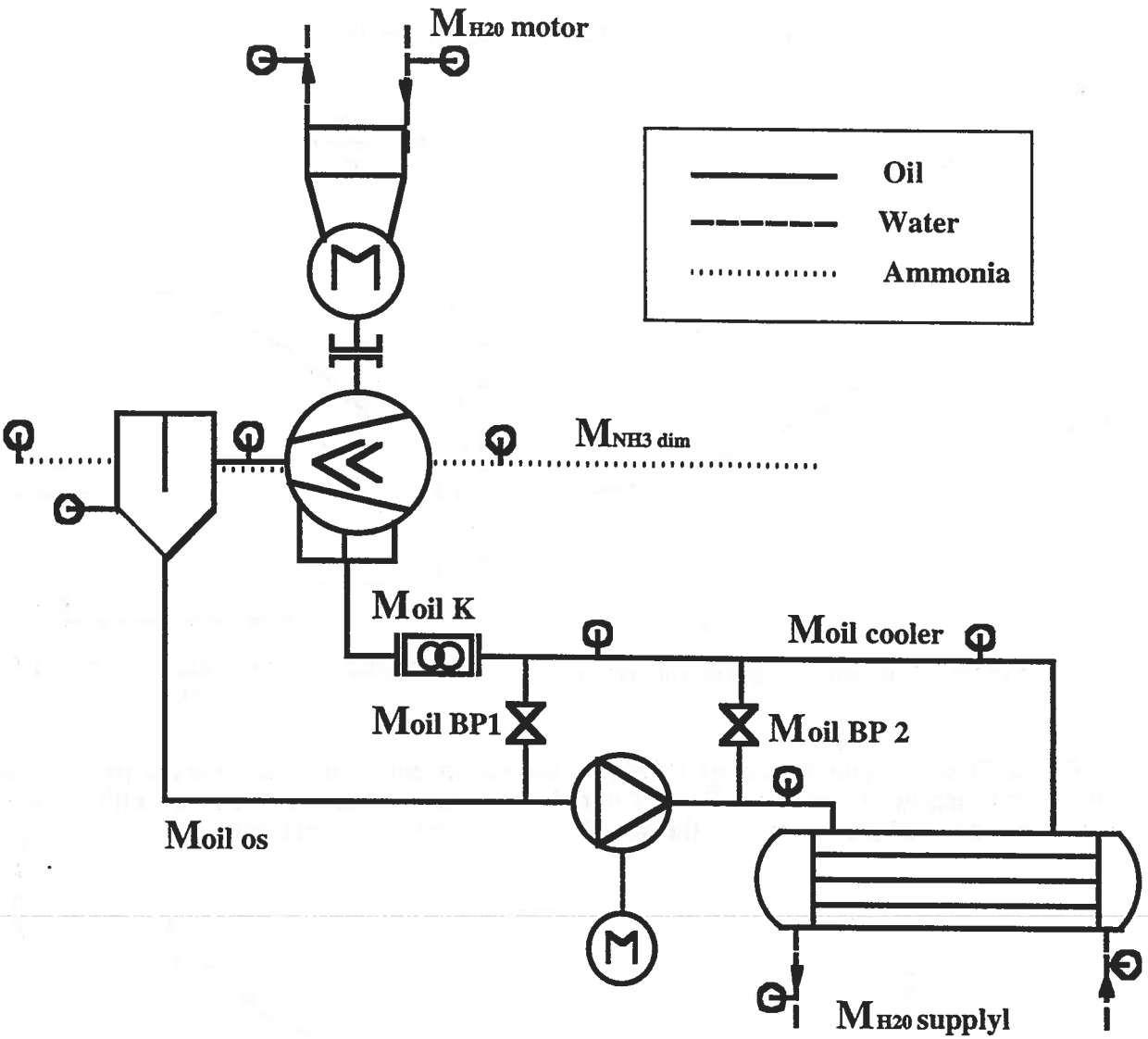

Figure 27: Sketch of the oil circuit

The different equations to find the different oil states are shown in appendix II

The first law balance on the oil cooler is:

$$\dot{W}^{-}_{OC_{H_2O}} + \dot{Q}^{-}_{loss} = \dot{W}^{+}_{OC_{oil}} \qquad (22)$$

and the second law:

$$\dot{E}^{+}_{W_{oil}OC} = \dot{E}^{-}_{W_{H_2O}OC} + \dot{L} \qquad (23)$$

The first law efficiency on the oil cooler is bigger than 100%, this error is mainly due to two elements. The first one is the supply flow that is not correct and indicates a too high quantity. The other source of error is the relationship of the mass density that seems incorrect when comparing the value given by the oil producer.

The efficiencies on the oil cooler are (Figure 28 and Figure 29):

$$\eta_I = \frac{\dot{W}^-_{OC_{H_2O}}}{\dot{W}^+_{OC_{oil}}} \qquad \eta_{II} = \frac{\dot{E}^-_{W_{H_2O}OC}}{\dot{E}^+_{W_{oil}OC}} \qquad (24)$$

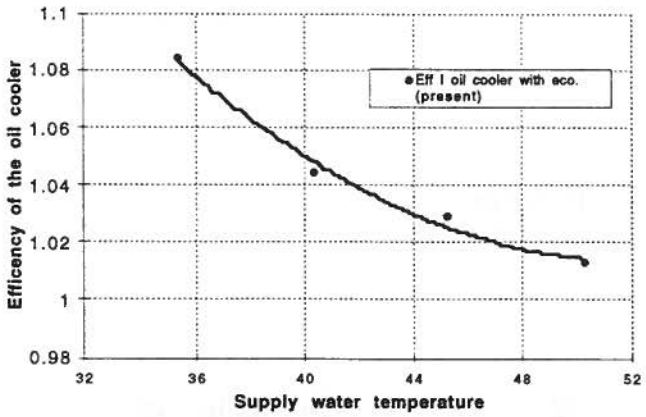

Figure 28: Efficiency of the oil cooler

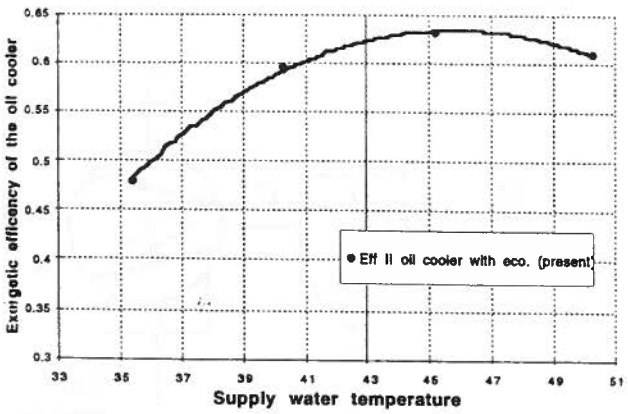

Figure 29: Exergetic efficiency of the oil cooler

Figure 28 shows that the energy balance is not very accurate and the error has probably to do with an overestimation of the water flow. The only comparison that can be done with reasonable care between initial and present tests is the heat flux on the supply water (Figure 30).

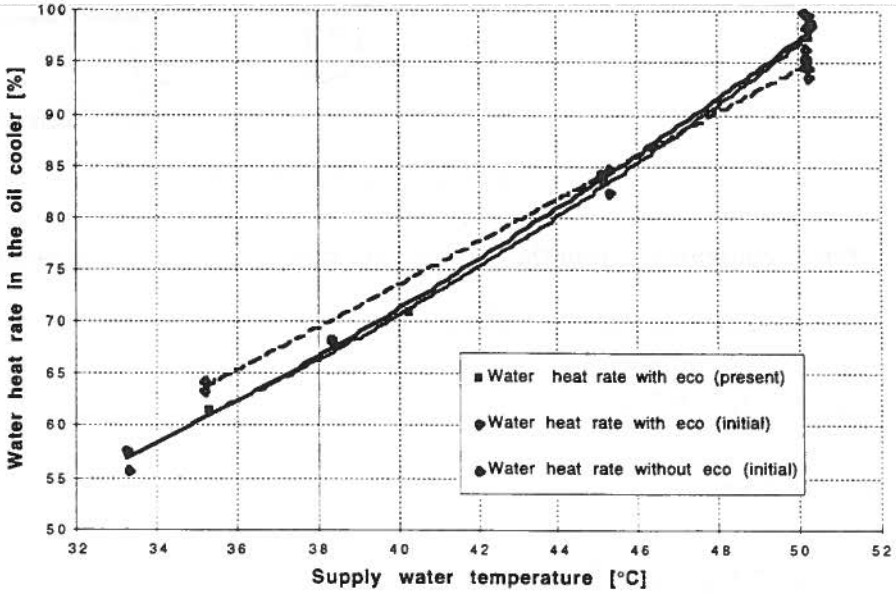

Figure 30: Comparison of the heat water flux of the oil cooler

The water rate power varies between +4% and -4%. Figure 31 and Figure 32 show that at low supply water temperature it is the water flow that induces a difference of oil heat rate and at 50°C the increase of water temperature is due to the low temperature at the entry of the supply water.

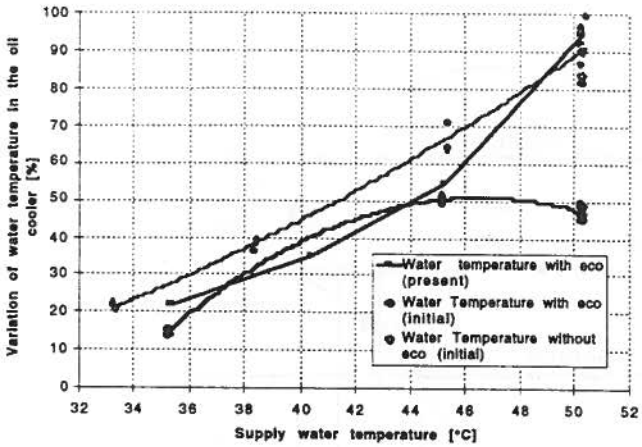

Figure 31: Variation of oil temperature in the oil cooler

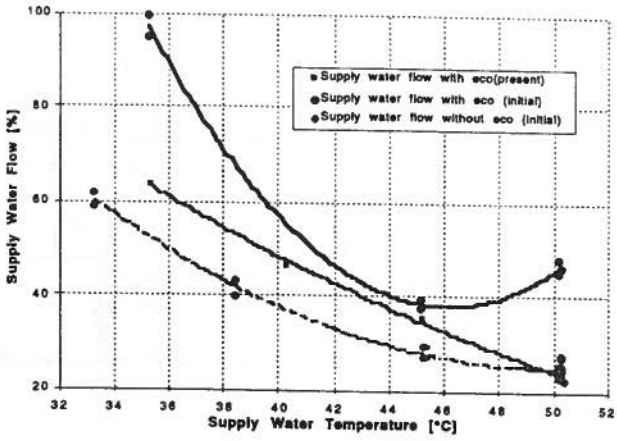

Figure 32: Supply water flow in the oil cooler

4.3 Compressor

In the chapter 3.4 an increase of electricity power has been noticed between present and initial tests.

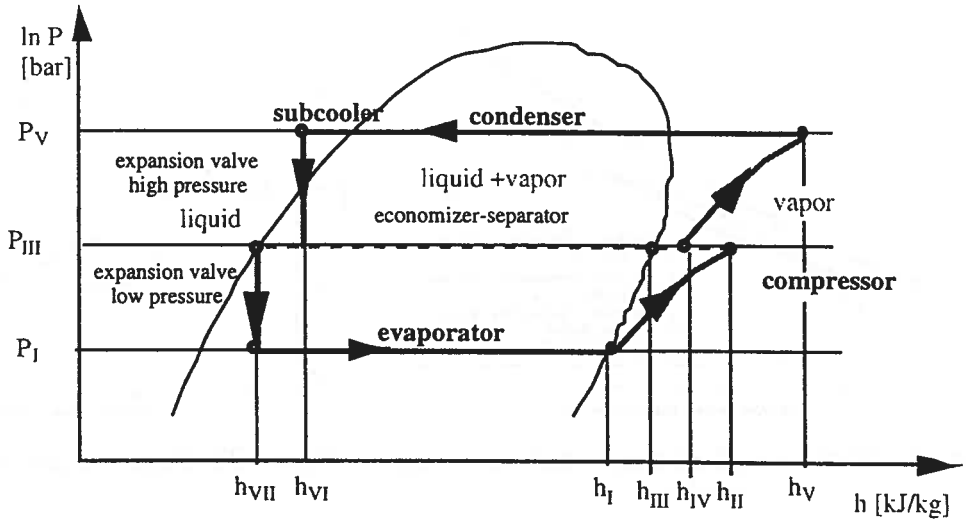

Figure 33: Ammonia cycle working with the economizer.

The first law is:

$$\dot{W}^{-}_{NH_3\,K} + \dot{W}^{-}_{oil\,K} + \dot{Q}^{-}_{loss} = \dot{E}^{+}_{El\,K} \qquad (25)$$

with an ammonia transformation power $\dot{W}^{-}_{NH_3\,K}$:

$$\dot{W}^{-}_{NH_3\,K} = \dot{M}_{NH_3\,dim}\, h_{NH_{3I}} + M_{NH_3eco}\, h_{NH_{3III}} - \dot{M}_{NH_3\,tot}\, h_{NH_{3V}} \qquad (26)$$

The oil power transformation $\dot{W}^{-}_{oil\,K}$ is calculated with the injection temperature of the oil into the compressor and the temperature of the ammonia at the exit of the compressor (the ammonia and the oil are considered at an equilibrium state at the exit of the compressor). The oil heat rate includes the heat required to cool down the bearings.

The electrical power of the compressor in equation 25 is taken as the shaft power. The efficiency of the motor furnished by the constructor ABB is 96.5%. If it is calculated on the basis of the thermal loss we get an average efficiency of 97.3%. The other losses are on different forms (mechanic, ventilation, electromagnetic) [12]. The initial measurements did not allow the calculation of the thermal losses on the motor, so an efficiency of 96.6% was estimated.

Thermal loss:

$$\dot{Q}^{-}_{Motor} = \dot{M}_{Motor}.c_{p_{H_2O}}(T_{out} - T_{in}) \qquad (27)$$

The mechanical power to the shaft is:

$$\dot{E}^{+}_{shaft} = \varepsilon_{motor}\, \dot{E}^{+}_{El} \qquad (28)$$

The efficiency (Figure 34) is so:

$$\eta_I = \frac{\dot{W}^{-}_{NH3}}{\dot{E}^{+}_{shaft}} \qquad (29)$$

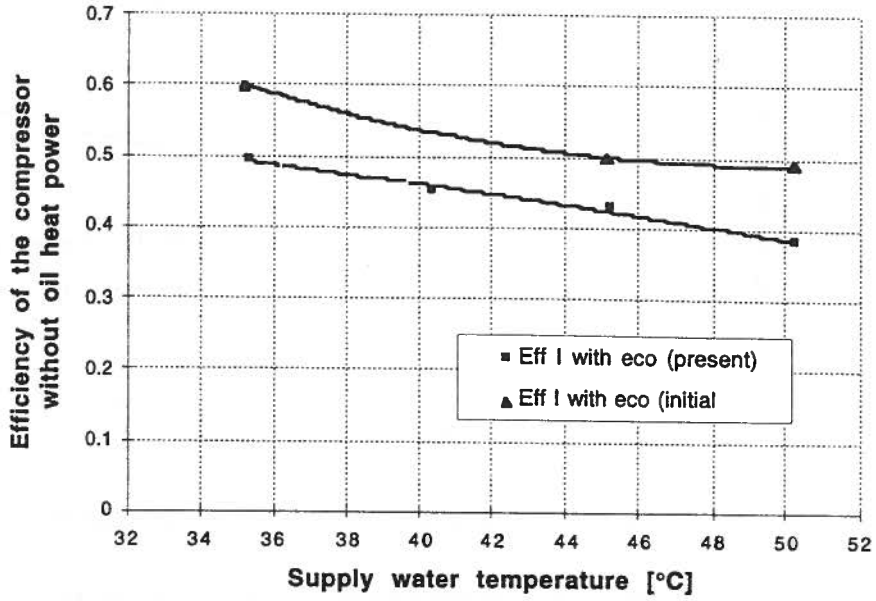

Figure 34: Efficiency of the compressor without oil heat power

Figure 34 shows an efficiency (not accounting for the oil) of the compressor decreases by 10%. Then the difference in efficiency is not entirely due to the augmentation of oil heat power. The ammonia heat Transformation power (enthalpy difference) (Figure 37) decrease of around 8% and the electrical power increases of around 13% (Figure 23).

For the exergetic balance:

$$\dot{E}^{+}_{e_{El}} = \dot{E}^{-}_{W_{NH3}\,K} + \dot{E}^{-}_{W_{oil}\,K} + \dot{L} \qquad (30)$$

with a transformation power of the ammonia $\dot{W}^{-}_{NH3}$:

$$\dot{E}^{-}_{W_{NH_3}K} = \dot{M}_{NH_3\,dim}\left((h_{NH_{3I}} - h_{NH_{3V}}) - Ta\,(s_{NH_{3I}} - s_{NH_{3V}})\right) + M_{NH_3eco}\left(h_{NH_{3V}} - h_{NH_{3III}} - Ta\left(s_{NH_{3V}} - s_{NH_{3III}}\right)\right) \qquad (31)$$

NB: The temperatures and the pressures at the exit of the compressor are considered as identical for the ammonia and the oil.

The exergetic efficiency (Figure 35) is:

$$\eta_{II} = \frac{\dot{E}^{-}_{W_{NH3K}} + \dot{E}^{-}_{W_{oil}}}{\dot{E}^{+}_{e_{shaft}}} \qquad (32)$$

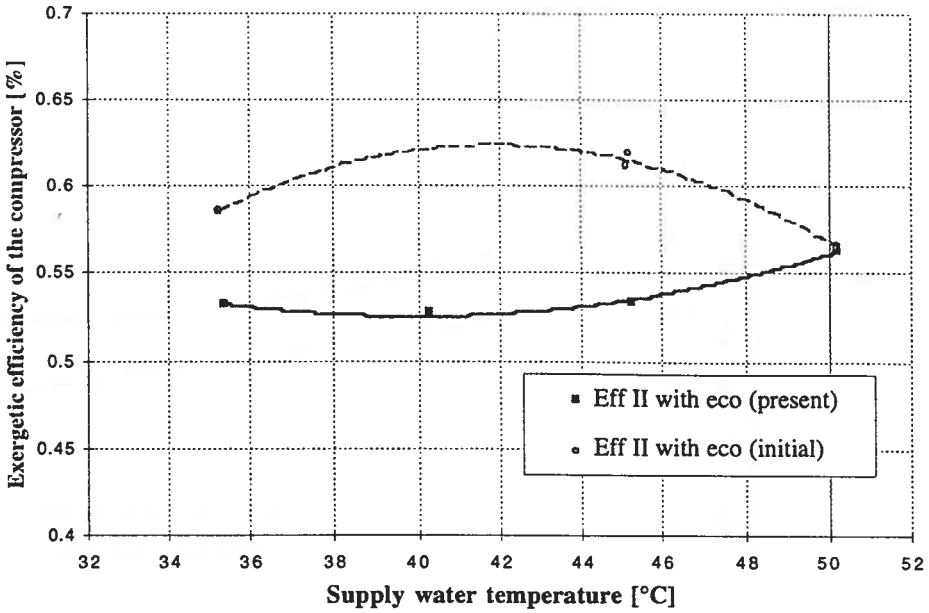

Figure 35: Exergetic efficiency of the compressor

To calculate the polytropic and isentropic efficiency of the compressor some hypothesis have to be made to calculate the unknowns of the compressor. The first one is that the system is divided in two parts, a low pressure (LP) part and a high pressure (HP) part. We will suppose they have an identical polytropic factor.

$$\eta_{LP} = \eta_{HP} \qquad (33)$$

The method to calculate the polytropic, isentropic efficiency and the unknowns of the compressor is shown in appendix III.

The isentropic efficiency of the compressor, when neglecting the kinetic energy in the suction and discharge ports, is:

$$\eta_s = \frac{E^{+}_{s}}{\sum \dot{M}^{+}_{i}\,\Delta h_i + \dot{Q}^{-}_{oil\,K}} = \frac{\sum \dot{M}_{i_{NH_3}}\,\Delta h_{i_s}}{\sum \dot{M}^{+}_{i}\,\Delta h_i + \dot{Q}^{-}_{oil\,K}} \qquad (34)$$

with $\sum \dot{M}^{+}_{i}\, h_i = M_I(h_{II} - h_I) + M_{IV}(h_V - h_{IV})$ for the compressor with the economizer port

The cooling effect of the oil is calculated on the basis of an average specific heat between the injection temperature and the discharge temperature. Results (Figure 36) show a decrease of the compressor isentropic efficiency on the order of 2 to 3 percentage points which partly explains the exergetic efficiency drop of the heat pump itself. This efficiency decrease is likely to be linked to rotor wear increasing the internal leakage. This can also be observed with the reduced mass flows observed in the recent tests for similar pressure ratios. An analysis is still under way to determine

from the data base of the measured results if there is evidence of increased mechanical losses. The thermal energy recovered from the electric motor corresponds to the electric efficiency given by the motor supplier and there is no data from the initial tests that indicates an eventual degradation.

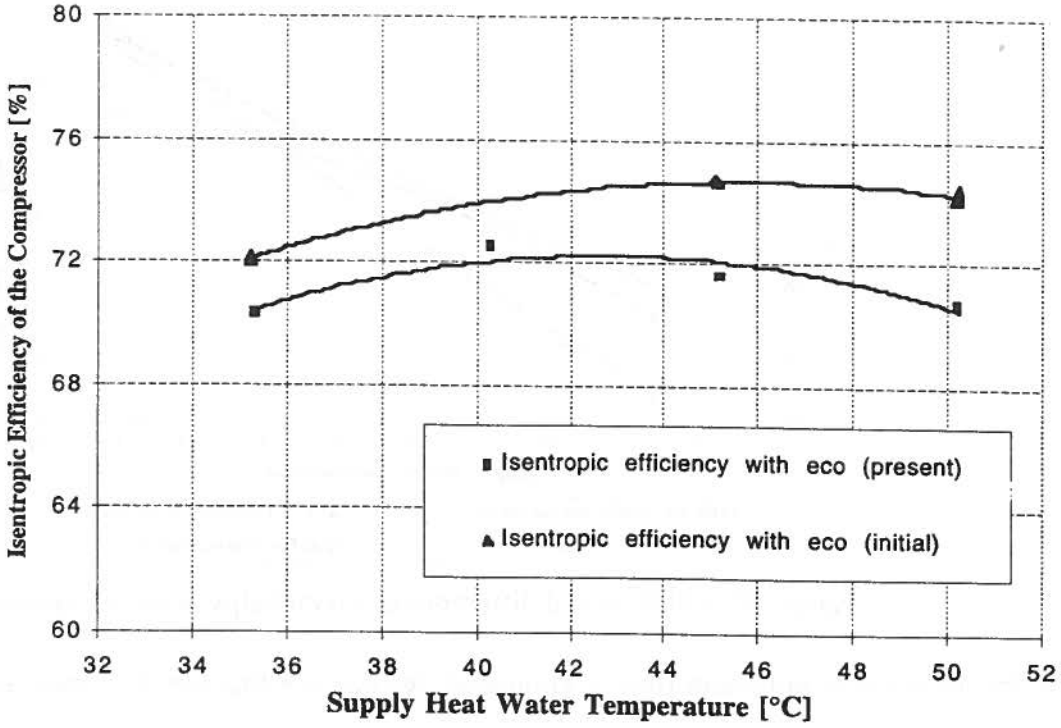

Figure 36: Isentropic efficiency of the compressor

The difference between present and initial tests is due to different factors. The electrical power during the present tests give a difference of around 7% (Figure 23). The heat rate for the oil is approximately 5% bigger during the present tests. For the ammonia transformation rate the difference varies from 8% for the temperatures from 35 to 45°C to 14% at 50°C. (Figure 37)

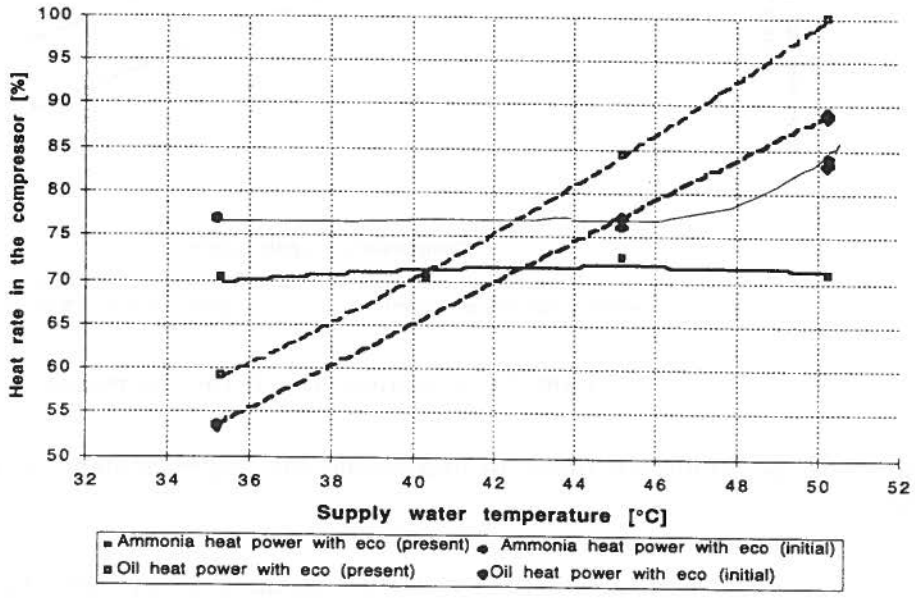

Figure 37: Ammonia and oil heat power in the compressor

The augmentation of oil heat rate is due to an augmentation of oil flow (+5%) in the compressor and also to a variation of enthalpy (+3% to -1%) (Figure 38). This augmentation of oil heat power is in relationship with the augmentation of ammonia heat power.

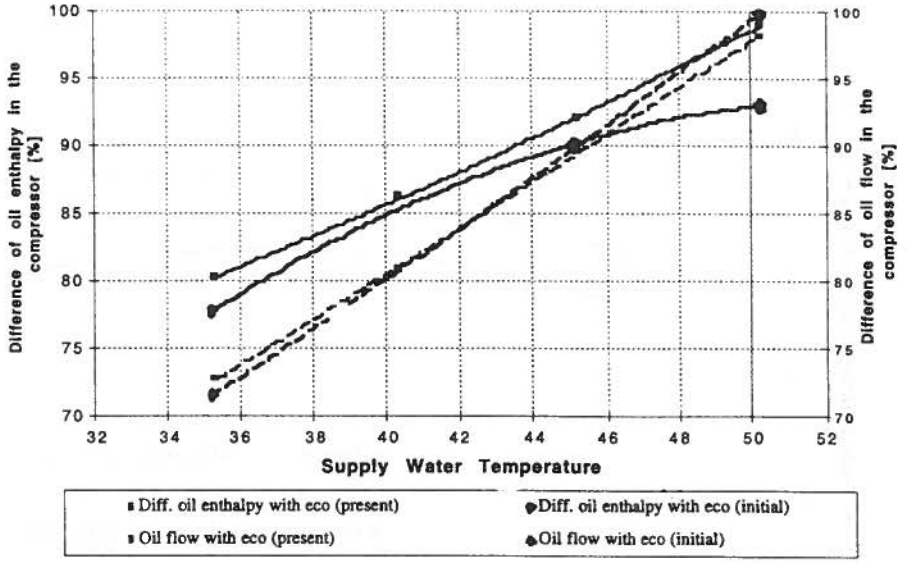

Figure 38: Oil flow and difference of oil enthalpy in the compressor

If the variation of ammonia flow is compared, we can see that the difference is constant (Figure 39).

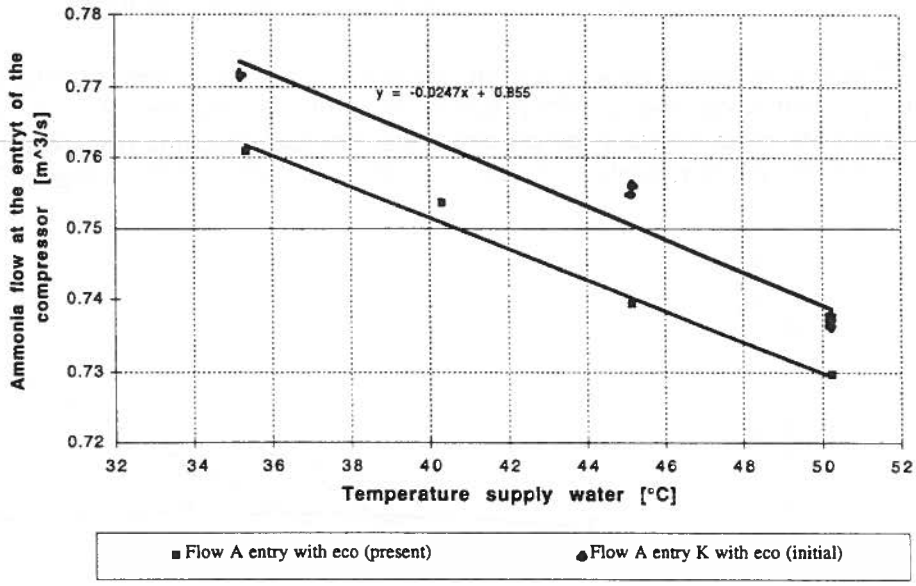

Figure 39: Ammonia flow in the compressor

Different suppositions are made to understand the larger demand of power on behalf of the compressor:

- Leakage in the compressor

This phenomena can be seen with the diminution of ammonia flow. The ammonia and oil temperatures have increased at the exit of the compressor.

- Mechanical defects: vibrations in the compressor, coupling

4.4 Evaporator

The evaporator is a spray-type shell-and-tube exchanger. It is composed of a tube bundle in the lower half of the shell which is sprayed with ammonia by nozzles located in the upper part of the shell (Figure 40). The accumulator underneath is used among other things as a receiver to collect the ammonia when the heat pump is stopped, and to prevent the ammonia from freezing the water in the tubes.

Two pumps, only one of which is normally in operation (the commissioning test showed that the calculation of the pressure drop was over-estimated by the supplier) gives a flow rate of four to five times the boiling rate.

Main external dimension [11]:

External diameter of the shell	1.9 m
Internal diameter of the shell	1.8 m
Length without water box	6.0 m
Volume of ammonia	12300 litre
Volume of water	6260 litre
Capacity NH_3 max.	1050 kg
Capacity NH_3 min.	800 kg
Four-pass exchanger with plain carbon steel tube	
Water fouling factor	$0.5*10^{-4}$ m^2K/W
Oil fouling factor	0 m^2K/W
Water pressure-drop (constructor)	60 kPa
Water pressure-drop (average calculated with the present tests)	9.3 kPa
Thermodynamic loss (average calculated with the present tests)	-6.57 kW
Pinch temperature (average calculated with the present tests)	2.87 °C

Heat exchanger tubes:

Number	1270
Type	bare tube
Diam. ext. * thickness	25 * 1.5 mm
Length	6000 mm
Material	stainless steel W-No 1.4571 (V4A)

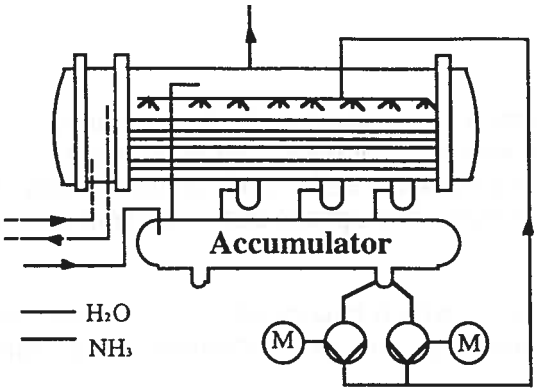

Figure 40: Sketch of the evaporator

For the evaporator the first law gives, the following equation:

$$\dot{W}^{-}_{NH_3} = \dot{W}^{+}_{H_2O} + \dot{E}^{+}_{PA} + \dot{Q}^{+}_{room} \qquad (35)$$

then the efficiency (Figure 41) is:

$$\eta_I = \frac{\dot{W}^{-}_{NH_3}}{\dot{W}^{+}_{H_2O} + \dot{E}^{+}_{PA} + \dot{Q}^{+}_{room}} \qquad (36)$$

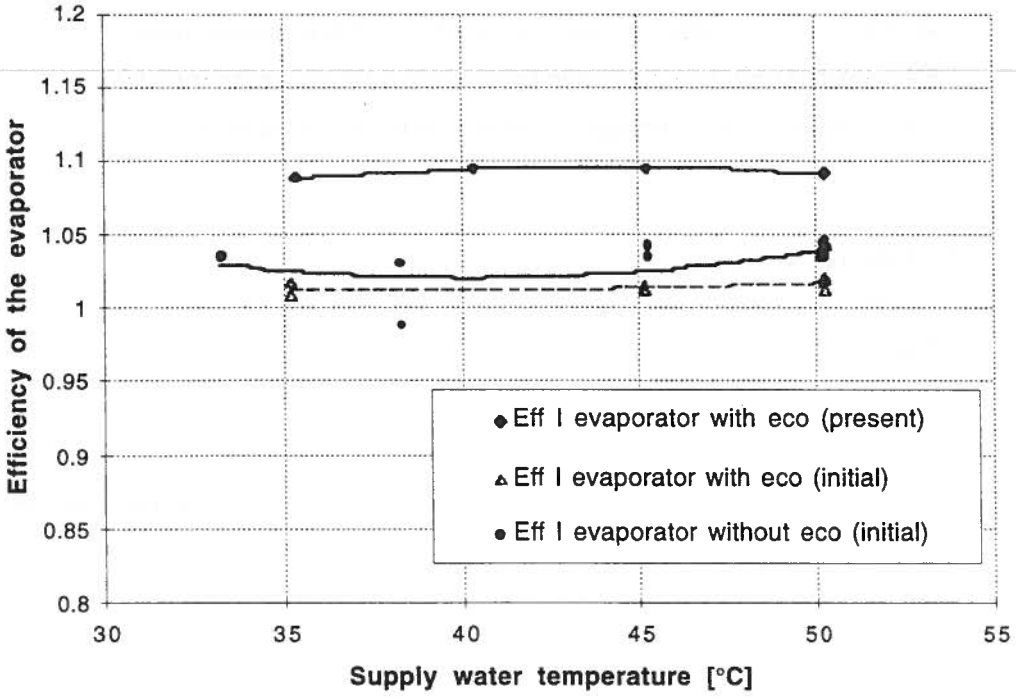

Figure 41: Efficiency of the evaporator

Figure 41 shows that the energy balance is not very accurate. The cause of these errors seems to come from the water flow meter and the precision of the temperature sensors. This phenomena can be seen by comparing the ammonia and water heat rates. This difference is approximately 5%. This difference increases for the water; it becomes as higher as 12% (Figure 42).

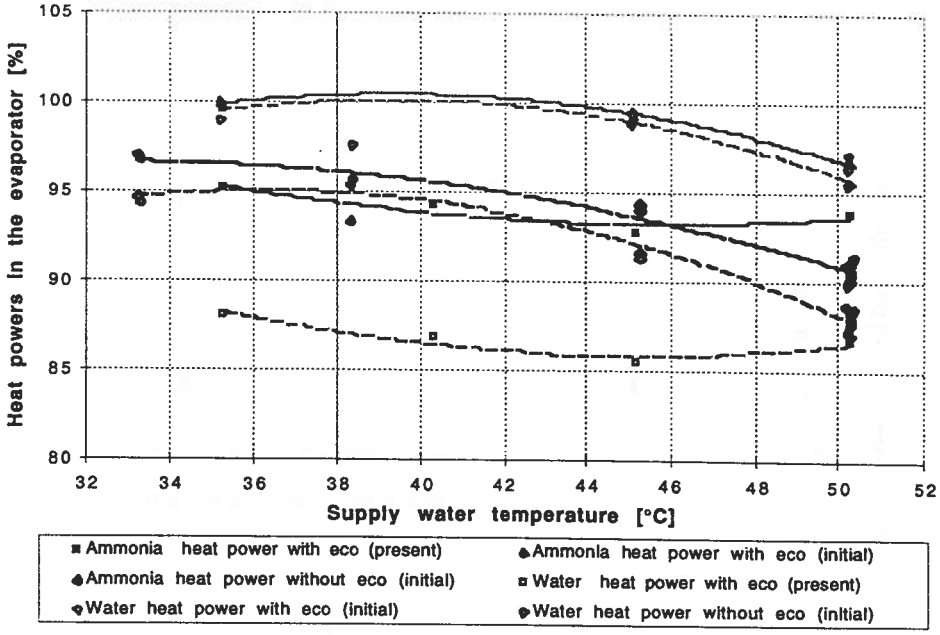

Figure 42: Difference of heat power on the ammonia and water side

The water flow is not regulated. The flow depends on the system of pumps near the lake. These pumps supply the heat pumps as well as industrial water for the cooling system of the buildings and for laboratory equipment. When the heat pumps are working the water flow for the evaporator is situated between two limits: if the flow is below the lower limit (210 [kg/s]) a supplementary pump is switched on. In the contrary, if the flow is too high (over 280 [kg/s]) one of the pumps is switched off. When the different flows are compared (Figure 43) this effect can be seen; there is no relationship between the different measurements. The measurements are dispersed. Only measurements that were made approximately during the same period are similar.

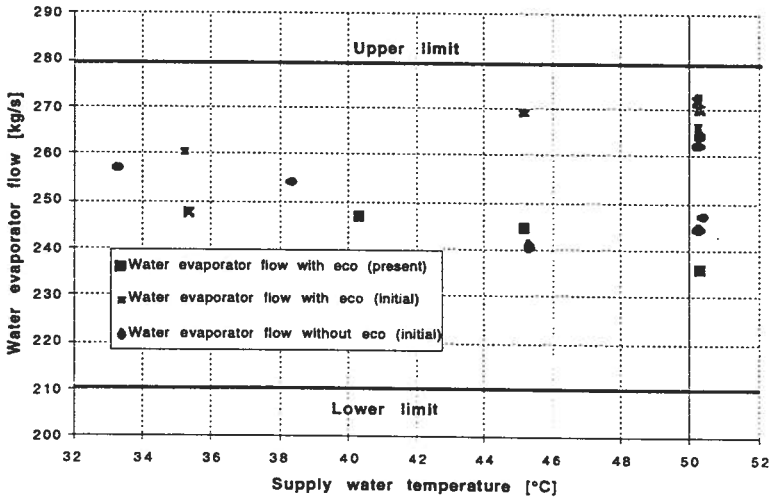

Figure 43: Water flow in the evaporator

As a comparison of heat power is not possible due to the defect of the flow meter, another comparison with the pinch temperature is done to know how the evaporator has evolved. Figure 44 shows the variation of the pinch temperature difference between the saturation temperature of the ammonia and the exit lake water temperature. It indicates a degradation of the heat transfer mainly due to fouling which, after compressor losses, is the second most important source of the reduction in heat pump performances.

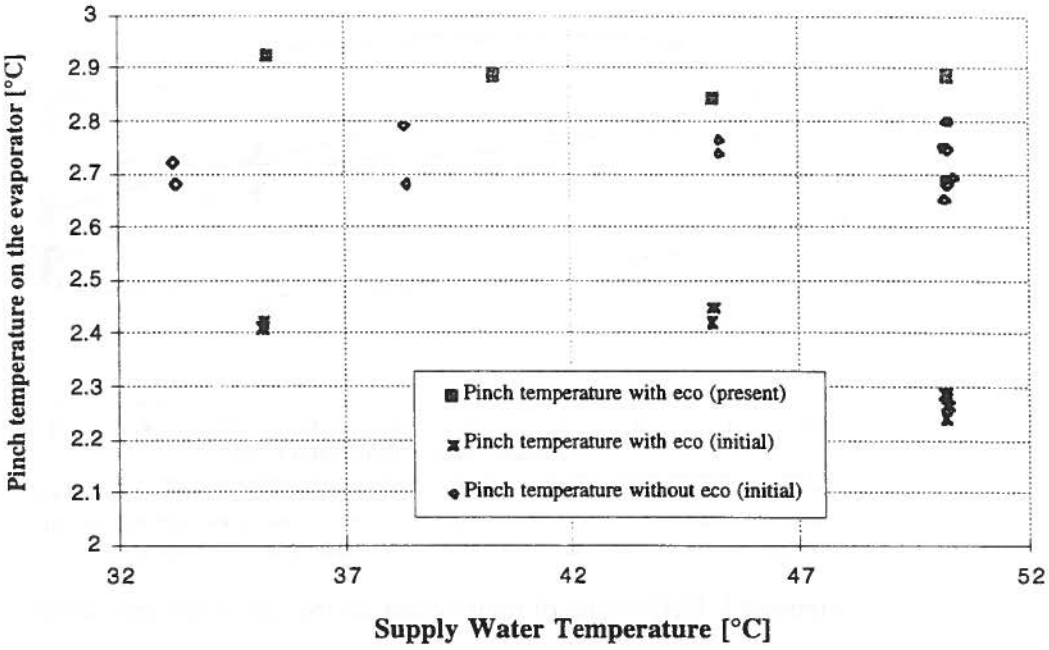

Figure 44: Pinch temperature in the evaporator

5. CONCLUSIONS

Detailed tests undertaken over an entire season after eleven years of operation allow the following observations:

- In spite of reduced performance of some of its components (compressor, evaporator fouling, inert gases) the ammonia heat pumps still demonstrate a coefficient of performance higher than 4 over all the heating season. This would translate into a virtual heating first law efficiency of 160% of the total system combining heat pumps and cogeneration units, proving the interest of this kind of technology integration.

- Due to relatively high price of electricity and low price of oil, present operation strategies tend to reduce the overall first law efficiency of the plant with a higher than expected use of the cogeneration units and a correspondingly lower use of the heat pumps. With these strategies the capacity of the storage tanks is not sufficient to avoid gas by-passing of the gas turbines heat recovery units. However, new strategy approaches with predictive control could improve the efficiency of storage tank use.

Xavier PELET

Lausanne,the 5th november 1997

6. SYMBOLS

A	area	[m^2]
COP1/2/3	energetic efficiency (first law)	[–]
η_I	(or Eff I)energetic efficiency (first law)	[–]
η_{II}	(or Eff II) exergetic efficiency (second law)	[–]
Cp	isobar specific heat	[J/kg.K]
Cv	isochore specific heat	[J/kg.K]
d	diameter	[m]
$\dot{E}$	technical power rate	[W]
$\dot{E}_e$	work copower	[W]
$\dot{E}_q$	heat copower	[W]
$\dot{E}_w$	transformation copower	[W]
g	gravity	[m/s^2]
h	enthalpy	[J/kg]
h	hours	[hour]
L	length	[m]
$\dot{M}$	flow	[kg/s]
Nu	Nusselt number $= \alpha\, d/\lambda$	[–]
P	pressure	[Pa]
Pr	Prandtl number = $Cp\, \mu/\lambda$	[–]
PR	Pressure ratio	[–]
$\dot{q}$	tube wall heat flux	[W/m^2]
$\dot{Q}$	heat transfer rate	[W]
Ra	Rayleigh number	[–]
Re	Reynolds number	[–]
R_{th}	thermic resistance	[K/W]
s	entropy	[J/kg K]
T	temperature	[°C] or [°K]
Ta	exterior temperature	[°C]
ThB	thermic balance	[–]
u	internal energy	[J/kg]
$\dot{W}$	transformation power	[W]
w	speed	[m/s^2]

x	vapour quality	[–]

Greek Letters

α	average heat transfer coefficient	[W/K m^2]
α_σ	polytropic calorific factor	[-]
α_v	isochore factor T/P	[-]
β	volumetric thermal coefficient	[1/K]
β_p	isobar factor T/v	[-]
Γ	mass flow rate in both side and per unit axial length	[kg/(m.s)]
γ_t	isotherm factor v/P	[-]
γ_σ	polytropic calorific factor	[-]
ε	emissivity	[-]
η	polytropic factor	[-]
Λ	calorific factor	[-]
λ	thermal conductivity	[W/K.m]
ν	kinetic viscosity	[m^2/s]
μ	dynamic viscosity	[kg/s m]
ρ	mass density	[kg/m^3]
v	specific volume	[m^3/kg]
σ	Stefan-Boltzmann constant	[W/m^2 K^4]

Subscripts:

SC	subcooler
Acc	accumulator
BP	by-pass
cond	conduction
conv	convection
C	condenser
dim	diminution (concerns the ammonia flow without the economizer flow)
eco	economizer
El	electric
ext	exterior
Ev	evaporator

H_2O	water
HP	heat pump
in	entry
K	compressor
LP	low pressure
NH_3	ammonia
OC	oil cooler
OS	oil separator
out	exit
L	liquid
PO	oil pump
PA	pump ammonia
rad	radiation
s	isentrope
tot	total
tr	transition
V	vapour
σ	polytrope

7. BIBLIOGRAPHY

[1] FAVRAT, D. (H)CFC Replacement: a Glance at Swiss Activities Including Boiling Research. IEA, Sittard Netherlands, September 1994.

[2] A. TASTAVI ET AL., *The Heating Network of EPFL with Cogeneration and Heat Pump Facilities*, Int. Conf. on Conventional & Nuclear District Heating, Lausanne, Mars 1991

[3] VON SPAKOVSKY M.R., CURTI V., *The performance Optimization of a Cogeneration / Heat Pump Facility*, Journal of Engineering for Gas Turbines and Power, ASME, vol 117, No1, PP 2-9, 1995

[4] INFO-ENERGIE, Département des travaux publics, de l'aménagement et des transports du canton de Vaud, novembre 1993

[5] D. FAVRAT, A.TASTAVI, *Experience with 3.9MWth Ammonia Heat Pumps.* AIE Workshop on Compression Systems with Natural Working Fluids. Trondheim Oct 1995

[6] Scartezzini J-L and Co, *Application des methodes stochastiques: dimensionnement et regulation*, Projets NEFF 349/FN 2.331-0.86, EPFL, Lausanne, 1987-1989

[7] ASHREI Handbook, *FUNDAMENTALS*, pp 17.44-17.45, S.I. Edition, Atlanta USA, 1993

[8] BREOX, *Fluids and Lubrificants*, Information revue, May 1995

[9] F. P. Incropera, D. P. De Witt, *Fundamentals of Heat and Mass Transfer*, 3rd ed., p 496, Singapore, 1990

[10] L.BOREL, *Thermodynamique et Energétique*, Presses Polytechniques Romandes, Lausanne, 1984

[11] Sulzer documentation

[12] CHATELAIN, J. Machines électriques, *Traité d'électricité*, Volume X, Presses Polytechniques Romandes,Lausanne, 2nd ed, 1989.

Different people have contribuated by gathering the various type of informations of this present report. The authors express their thanks to:
J. Schmid, regulation specialist, CCT
H. Colomb, electricity service of the EPFL
B. Immer, service for the construction and buildings
J. Videla, exploitation service of theEPFL

Appendix

I. Method of calculation

To verify the method of calculation, a comparison of the total efficiency calculated by Sulzer and the one calculated by the LENI is done. This calculation was made separately. LENI does not possess the calculation codes used by Sulzer and vice versa. Only the final results were given by Sulzer. This comparison shows that there is no difference between the two methods (Figure 1).

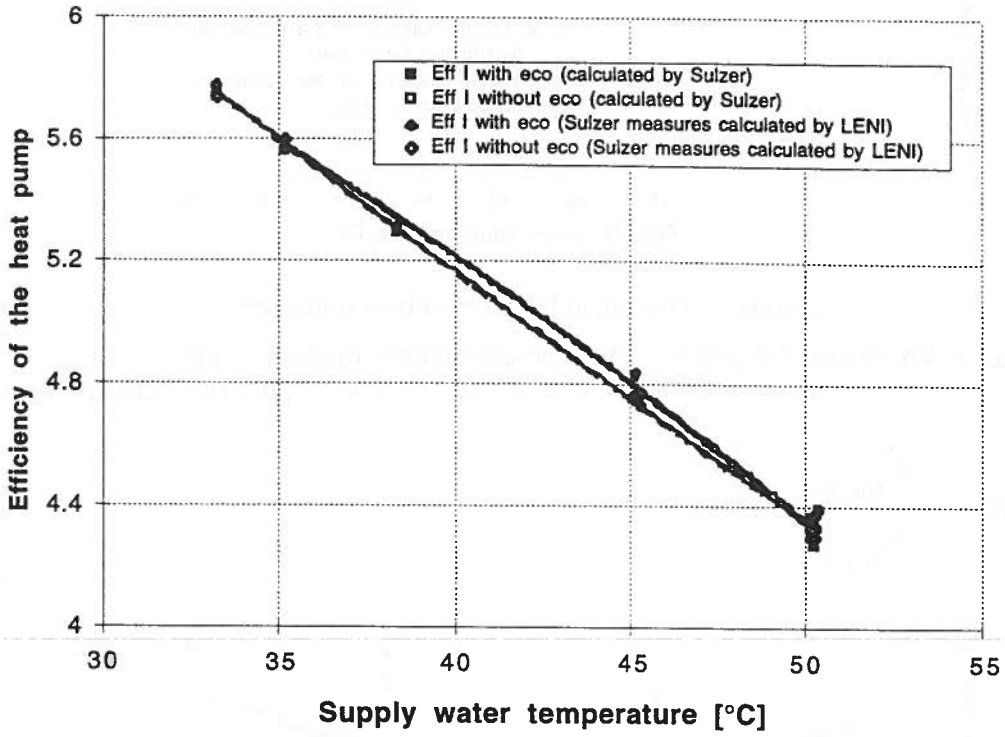

Figure 1: Comparison of the method of calculation of COP1 between LENI and Sulzer

To compare the results concerning the condenser, the report uses the following thermal balance (ThB_C) :

$$ThB_C = \frac{\dot{Q}^{+}_{NH_3\,C}}{\dot{Q}^{-}_{H_2O\,C}} \qquad (1)$$

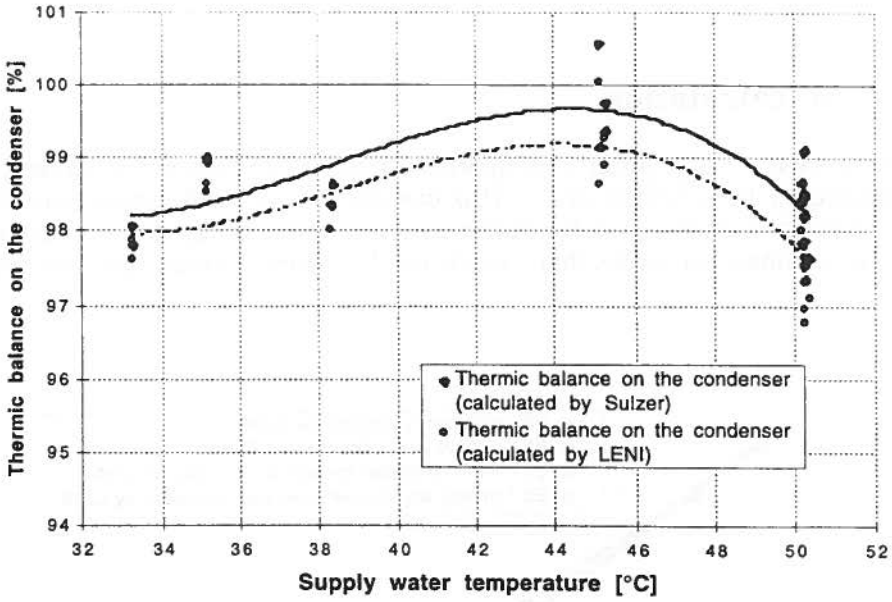

Figure 2: Thermical balance on the condenser

The difference is lower than 0.2 percent. Thus the calculation model is correct.
A comparison of the method of calculation is also done on the evaporator (ThB_{EV}) (Figure 3).

$$ThB_{Ev} = \frac{\dot{W}^{+}_{NH_3\,Ev}}{\dot{W}^{-}_{H_2O\,Ev}} \qquad (2)$$

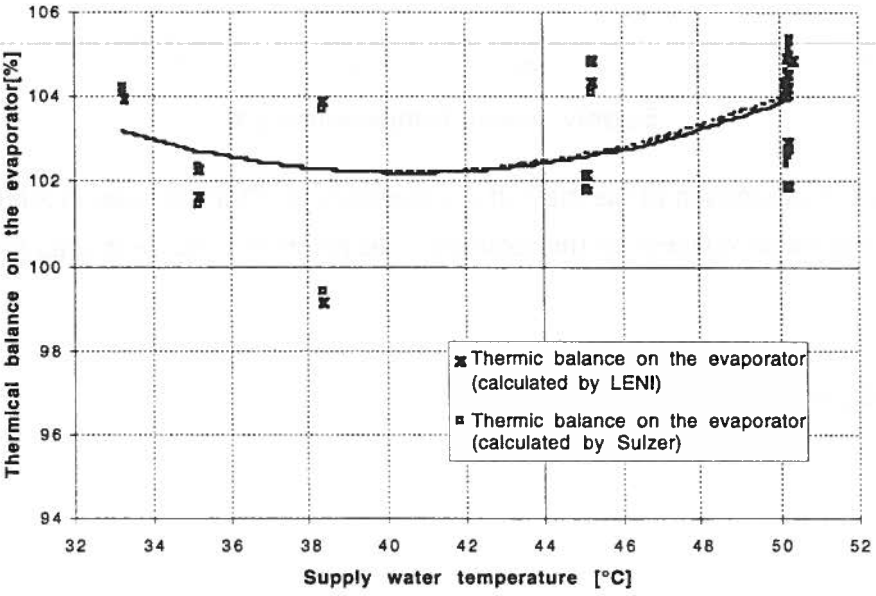

Figure 3: Comparison of the methods of calculation on the evaporator between Sulzer and LENI

The graph shows that there is almost no difference between the two ways of calculation.

II. Equations of the oil circuit

The flow balance on the first by-pass is:

$$M_{oil\ K} + M_{oil\ BP1} = M_{PO} \quad (3)$$

The thermal balance on the exit of the first by-pass is:

$$M_{oil\ K} \cdot h_{oil\ OS\ out} + M_{oil\ BP1} \cdot h_{oil\ BP1} = M_{oil\ PO} \cdot h_{PO\ in} \quad (4)$$

with $h = Cp_{oil} \cdot T_{oil}$ the equation becomes:

$$M_{oil\ K} \cdot Cp_{oil}\ T_{oil\ OS} + M_{oil\ BP1} \cdot Cp_{oil} \cdot T_{oil\ Kin} = M_{PO} \cdot Cp_{oil} \cdot T_{oil\ OCin} \quad (5)$$

by replacing the flow $M_{oil\ BP1}$:

$$M_{oil\ K} \cdot Cp_{oil} \cdot T_{oil\ OSout} + (M_{PO} - M_{oil\ K}) \cdot Cp_{oil} \cdot T_{oil\ Kin} = M_{PO} \cdot Cp_{oil} \cdot T_{oil\ OCin} \quad (6)$$

The oil temperature in the separator is not measured by LENI's sensors, but it is measured by the Sulzer's sensor. This temperature was deduced from Sulzer's results by estimating the heat loss in the oil separator from the temperature at the exit of the compressor.

Note: Ammonia and oil are at the same thermodynamic state at the exit at the oil compressor.

$$M_{oil\ K} \cdot Cp_{oil} \cdot T_{NH3\ Kout} + (M_{PO} - M_{oil\ K}) \cdot Cp_{oil} \cdot T_{oil\ Kin} = M_{PO} \cdot Cp_{oil} \cdot T_{oil\ OCin} \quad (7)$$

Finally we get:

$$M_{PO} = \frac{M_{oil\ K} \cdot (T_{NH_3 K_{in}} - T_{oil\ K_{in}})}{T_{oil\ OC_{in}} - T_{NH_3 K_{in}}} \quad (8)$$

At the exit of the second by-pass the flow balance is:

$$M_{oilOC} + M_{BP2} = M_{PO} \quad (9)$$

In the second by-pass the thermodynamic state is as follow:

$$M_{oil\ OC} \cdot h_{oil\ OCout} + M_{BP2} \cdot h_{oil\ BP2} = M_{PO} \cdot h_{oil\ Kin} \quad (10)$$

By replacing enthalpy and flow we get:

$$M_{oil\ OC} \cdot Cp_{oil} \cdot T_{oil\ OCout} + M_{BP2} \cdot Cp_{oil} \cdot T_{oil\ OCin} = M_{PO} \cdot Cp_{oil} \cdot T_{oil\ Kin} \quad (11)$$

$$M_{oil\ OC} \cdot Cp_{oil} \cdot T_{oil\ OCout} + (M_{PO} - M_{oil\ OC}) \cdot Cp_{oil} \cdot T_{oil\ OCin} = M_{PO} \cdot Cp_{oil} \cdot T_{oil\ Kin} \quad (12)$$

With these two equations, the flow in the oil cooler exchanger can be deduce:

$$M_{oilOC} = \frac{M_{PO} \cdot (T_{oilK_{in}} - T_{oilOC_{in}})}{T_{oilOC_{out}} - T_{oilOC_{in}}} \quad (13)$$

with M_{PO} calculated by equation (8).

III Compressor

To calculate the polytropic efficiency of the compressor some hypothesis has to be done to calculate the unknown of the compressor. The first one is that the system is divided in two parts, a low pressure (LP) part and an high pressure (HP) part. We will suppose they have an identical polytropic factor.

$$\eta_{LP} = \eta_{HP} \tag{14}$$

To calculate the polytropic factor some notions have to be introduced:
The polytropic transformation to go from a thermodynamic state one to two is:

$$\left(\frac{T_2}{T_1}\right) = \left(\frac{P_2}{P_1}\right)^{\alpha_\sigma} \tag{15}$$

$$\text{or } \alpha_\sigma = \ln\left(\frac{T_2}{T_1}\right) \Big/ \ln\left(\frac{P_2}{P_1}\right) \tag{16}$$

The isochore factor $$\alpha_v = \frac{P}{T}\left(\frac{\partial T}{\partial P}\right)_v \tag{17}$$

The isobar factor $$\beta_p = \frac{v}{T}\left(\frac{\partial T}{\partial v}\right)_p \tag{18}$$

The isochore specific heat $$c_v = T\left(\frac{\partial s}{\partial T}\right)_v \tag{19}$$

The isobar specific heat $$c_p = T\left(\frac{\partial s}{\partial T}\right)_p = \left(\frac{\partial h}{\partial T}\right)_p \tag{20}$$

The calorific factor $$\Lambda = 1 - \lambda = 1 - \frac{c_v}{c_p} \tag{21}$$

The isotherm factor $$\gamma_t = -\frac{P}{v}\left(\frac{\partial v}{\partial P}\right)_T \tag{22}$$

To go from state one to state two the way will be divided in "n" small segments

$$PR = \left(\frac{P_{out}}{P_{in}}\right)^{1/n} \tag{23}$$

$$\alpha_\sigma = \alpha_v \, \Lambda(1 + \beta_p(\eta - 1)) \tag{24}$$

$$\dot{E}_\sigma = \dot{M} v_1 \frac{P_1}{1 - \gamma_\sigma}\left(PR^{1-\gamma_\sigma} - 1\right) \tag{25}$$

The polytropic factor is:

$$\eta = \frac{dh}{vdp} = \frac{dh}{e_{\sigma}^{+}} \qquad (26)$$

if we make the hypothesis of a perfect gas the polytropic factor becomes:

$$\eta = \frac{\alpha_{\sigma}}{\Lambda} \qquad (27)$$

From the fundamental equation for an open system:

$$\delta e^{-} + \delta r = -vdP = -dh + \delta q^{+} + \delta r \qquad (28)$$

From the equation (28): $\delta e^{-} = -dh - \delta q^{-}$ (29)

$$\delta e^{+} = dh + \delta q^{-} \qquad (30)$$

The thermodynamic states are unknown just before the injection and just after the injection. To know them an iterative calculation has to be made.
Through a first estimation, it is possible to approximately know the thermodynamic state around the point of injection by making the hypothesis that there is no injection (Figure 4). This situation is the case without the economizer.

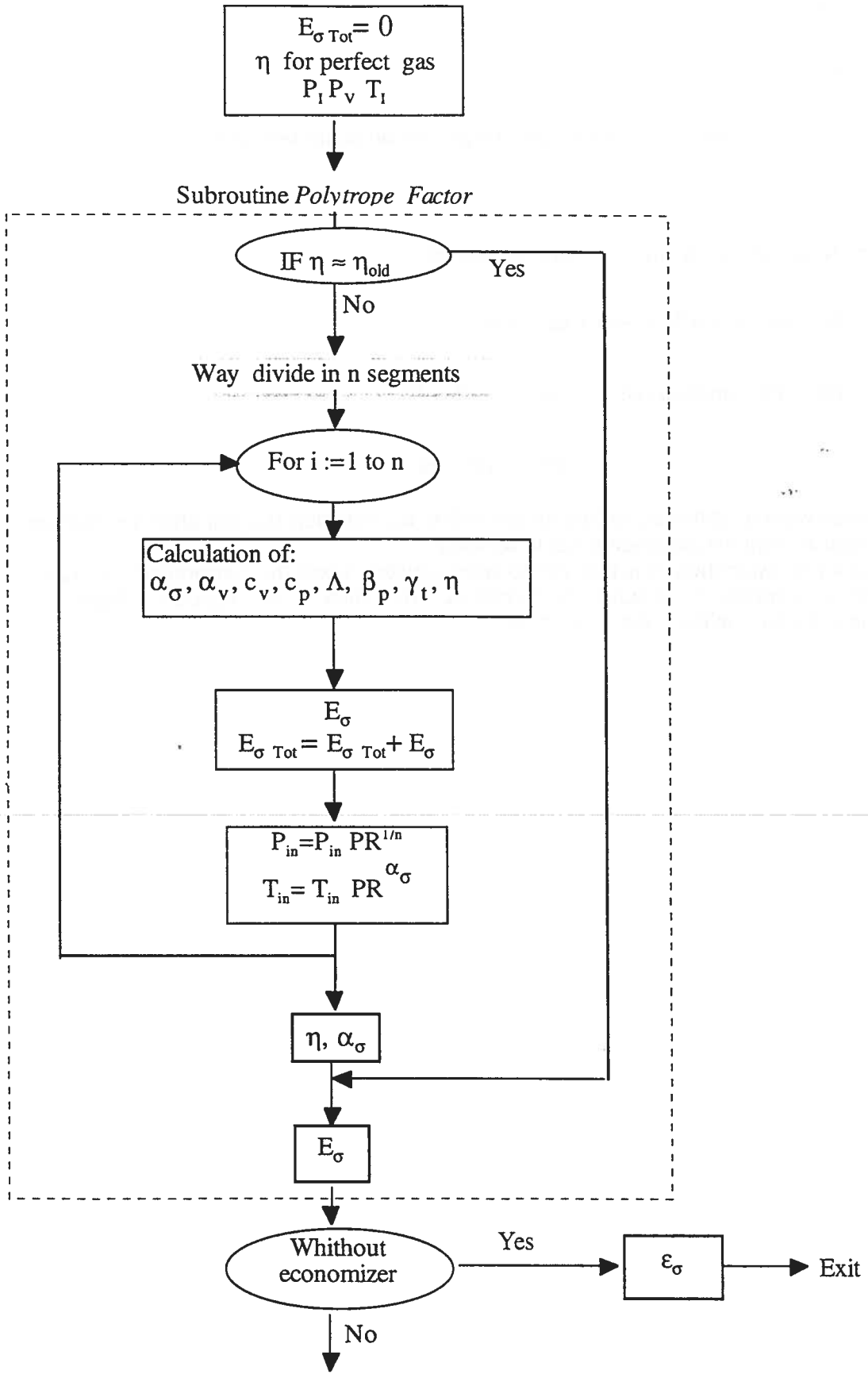

Figure 4: Iterative principal to find the polytropic factor of the compressor working without economizer port

The pressure before injection P_{II} is known, is the same as the one coming from the economizer (apart from the pressure-drop). It is also the same for the after pressure after the economizer.

$$P_I = P_{II} = P_{III} \qquad (31)$$

The iteration will consist to find the two states before and after injection with respect to the equation of mixing at the entry of the economizer into the compressor and considering an identical polytropic factor in the two parts of the compressor (Figure 5).
The mixing at the entry of the economizer in the compressor give according the first thermodynamic principal:

$$h_{III} \cdot M_{III} + h_{II} \cdot M_I = (M_I + M_{III}) \cdot h_{IV} \qquad (32)$$

The enthalpy h_{III} corresponds to the enthalpy at the saturated vapour in the economizer, therefore:

$$h_{IV} = \frac{h_{II} \cdot \dot{M}_{II} + h_{III} \cdot \dot{M}_{III}}{\dot{M}_I + \dot{M}_{III}} \qquad (33)$$

The unknown in the equation (33) is the state at the point II. To know it, an iteration has to be performed. This iteration is done by taking the initial values, those being the same values found in the case without the use of an economizer.

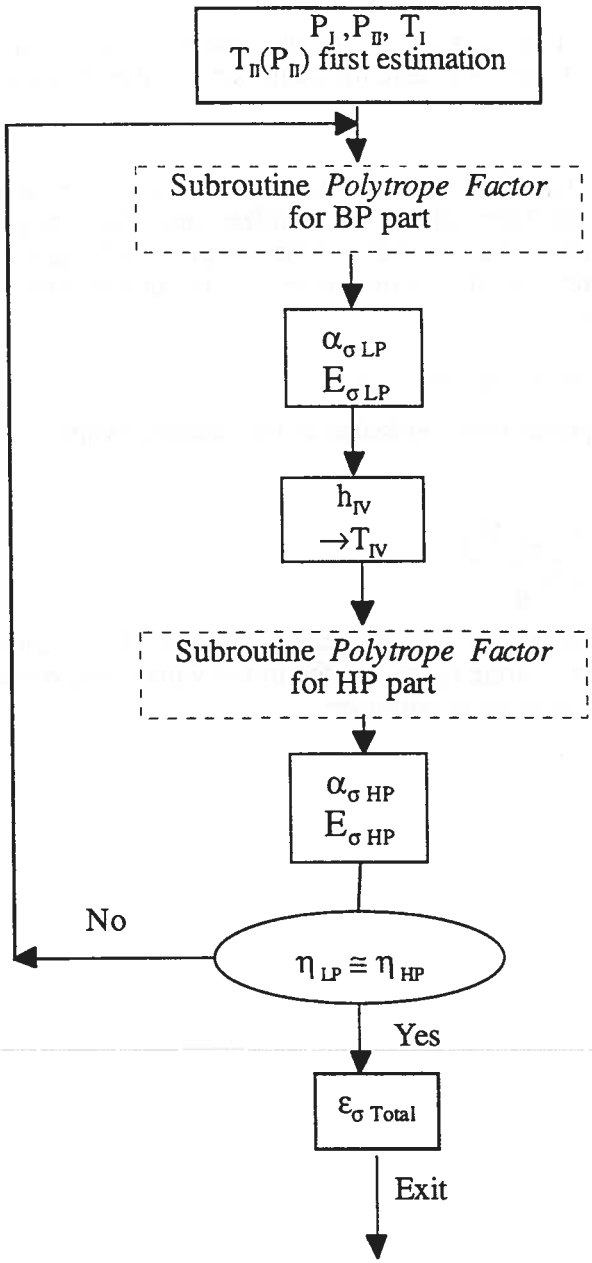

Figure 5: Iterative cycle to find the properties of a compressor with injection